Chemically Robust Covalent Organic Frameworks: Progress and Perspective

Xinle Li,[1] Songliang Cai,[2] Bing Sun,[3] Chongqing Yang,[1] Jian Zhang,[1] Yi Liu[1,*]

[1]The Molecular Foundry, Lawrence Berkeley National Laboratory, Berkeley, California 94720, United States
[2]School of Chemistry, South China Normal University, Guangzhou 510006, P.R. China
[3]School of Science, China University of Geosciences (Beijing), Beijing 100083, P.R. China

*Corresponding author: yliu@lbl.gov

Summary

Covalent organic frameworks (COFs) are functional porous crystalline "Molecular Legos" entirely composed of light elements and held together by covalent bonds. Their synthesis typically relies on the formation of reversible covalent bonds linking multivalent monomers. While the reversibility in linkage formation imparts error-correction and defect-healing that dictate crystallinity, the thermodynamic characteristics intrinsically limit the chemical stability of COFs and constrain their further applications. To overcome chemical stability issues, considerable research efforts have been devoted to developing robust COFs by strengthening covalent linkages, tailoring noncovalent interactions, and manipulating inherent properties of linkers. In this review, we first summarize the state-of-the-art development of chemically robust COFs, followed by scrutinizing the intriguing applications of chemically robust COFs in heterogeneous catalysis, environmental remediation, chiral separation, corrosive gas sensing, and lithium-ion batteries. We further present the major challenges and opportunities in future research directions and perspectives of chemically robust COFs.

Keywords: covalent organic frameworks, dynamic covalent chemistry, linkage, post-synthetic modification, stability

1. Introduction

Since the first seminar work by Yaghi's group in 2005,[1] covalent organic frameworks (COFs), an emerging class of crystalline porous materials constructed by stitching organic units together into extended periodic networks, have been at the forefront of porous materials research due to their unmatchable combination of high crystallinity, ultralow density (down to 0.17 g cm^{-3}), large surface areas (up to 5083 m^2 g^{-1}), adjustable pore size (up to 5.8 nm), and versatile molecular architecture.[2] These unique attributes have been successfully exploited to tailor COFs as an auspicious platform for a plethora of applications in areas including, but not limited to gas adsorption/separation, heterogeneous catalysis, chemical sensing, energy storage, and nano-electronics.[3-7]

COFs are typically synthesized by reticulating organic building blocks into extended networks in two or three dimensions (2D or 3D) by dynamic covalent chemistry, which empowers the crystallization of COFs by virtue of error-correction and self-healing processes. Unique insights regarding the crystallization process of COFs have been unraveled in the past decade. Taking imine-linked 2D COFs as an example, which consists the main body of reported COFs in terms of linkage, Dichtel's group uncovered that such COFs were formed through an amorphous-to-crystalline transition wherein an amorphous polymer rapidly precipitated, followed by a gradual crystallization into crystalline frameworks under dynamic conditions.[8,9] Such amorphous-to-crystalline reconstruction not only manifests the dynamic nature of COFs but also provides a viable route to preparing COFs from amorphous polymers.[10] Conventional solvothermal synthesis facilitates such transformations and has been the most dominant method for COFs preparation, though alternative innovative synthetic approaches have led to expeditious COF synthesis.[11]

To fuel the exploration of COFs in specialized applications, stability, including chemical, thermal, and mechanical stability, is deemed as one of the key prerequisites. Amongst these, chemical stability, pertaining to the ability to preserve long-range ordered structures in various chemical environments, e.g., solvents, acids, bases, and redox agents, is of great relevance for applications that relate to the transfer and storage of masses, charge carriers and ions. However, most COFs possess problematic chemical stability, perceived as the Achilles' heel of COFs, and cannot maintain their structural integrity in harsh chemical environments, thus severely constraining their practical utility in applications such as ion exchange, proton conduction, water desalination, and heterogenous catalysis that involve water/abrasive chemicals, varying pH and temperature.[12] The COF's instability mainly originates from the reversible linkage reticulating the organic units together, which imparts error-correction and defect-healing during bonds formation and yield the thermodynamically most stable crystalline architectures.[13] Once COFs are formed, however, the same reversible linkages that are required for crystallization also live in the framework. In spite of the

high bond energies due to the covalent nature, such linkages are susceptible to certain conditions, rending them as the weakest covalent links that greatly limit the intrinsic chemical stability of COFs.

In addition to the reversibility of covalent linkage, the chemical stability of COFs is also governed by two other factors, including supramolecular noncovalent interactions (e.g., hydrogen bonding and interlayer stacking forces) and inherent properties of linkers (e.g., steric and hydrophobicity) (Scheme 1).[14] In a typical *de novo* synthesis of COFs, a highly reversible linkage requires less energy input to afford a crystalline framework, yet it may be more susceptible to environmental conditions, as exemplified by boroxine or boronate ester-linked COFs. On the other hand, less reversible linkages require harsher conditions to reach thermodynamic equilibrium and are more prone to afford less ordered frameworks due to lower reaction selectivity and more side reactions, but the thus formed COF retains high chemical stability as exemplified by triazine-linked COFs. Schiff-base chemistry readily relieves such reversibility(stability)-crystallinity trade-off and imine-linked COFs constitute the largest members in COF chemistry to date. To further improve the stability of the prevalent imine-linked COFs, tailoring the supramolecular interactions and kinetically locking the reversible imine linkage by converting it into the robust irreversible unit via post-synthetic modification or *in situ* cascade reaction have been well implemented in COFs.[15,16] In addition, imparting surface hydrophobicity to COFs and steric hindrance adjacent to linkage through judicious selections of pre-designed building blocks or post-synthetic modifications effectively prevent the labile linkage from hydrolysis, thus enhancing the hydrolytic stability of COFs in the aqueous medium. Furthermore, developing new robust linkages that obviate the conventional reliance on dynamic covalent chemistry offers an appealing solution for the synthesis of chemically robust and functionally diverse COFs.

Over the past decade, various strategies have been proposed to construct chemically robust COFs, which significantly expand the scope, complexity, and applications of COFs. Herein, we aim to survey the recent advances in the preparation of chemically stable COFs and their applications. This review is not to duplicate the topics previously reviewed in the fields such as film,[17] separation,[18] chemical sensing,[19] catalysis,[20] etc., but to concentrate on the prevalent strategies to construct chemically robust COFs. This review begins with a summary of strategies that have been developed for improving COFs' chemical stability while scrutinizing the key factors in the synthesis of stable COFs. Next, the unique attributes of stable COFs and their promising applications in a broad array of areas including heterogeneous catalysis, environment remediation, chiral separation, corrosive gas sensing, and lithium-ion batteries are highlighted. In the end, unsettled challenges and future perspectives in this field are presented. Overall, this review is expected to offer guidelines for the synthesis of chemically robust COFs and accelerate the discovery of more robust advanced materials in the future.

2. Chemical Stability

To assess the chemical stability of COFs, a widely-adopted method is to immerse COF solids in various environments such as air, solvents (e.g., H_2O, organic solvents), acid (e.g., aqueous HCl, H_2SO_4, H_3PO_4, HNO_3, HF, triflic acid, trifluoroacetic acid, chromic acid), base (e.g., NaOMe, NaOH, KOH, NH_3, $NaHCO_3$), reducing agents (e.g., N_2H_4, $NaBH_4$, and $LiAlH_4$), oxidants (e.g., $KMnO_4$), organolithium reagents (e.g., *n*-BuLi, MeLi), and irradiations (e.g., light, γ-ray, and electron beam) at predesignated temperature (from ambient temperature to 100 ^oC). After soaking COFs for a certain time (ranging from several hours, days, months to even 1 year), COFs are isolated from the solutions, washed with organic solvents, re-activated under vacuum and subjected to routine structural characterizations such as powder X-ray diffraction (PXRD), N_2 adsorption-desorption measurements, and Fourier-transform infrared spectroscopy (FT-IR). Scanning electron microscope (SEM) and solid-state nuclear magnetic resonance (NMR) spectroscopy are also used albeit to a lesser degree. By comparing with the pristine materials, one is able to assess the chemical stability of COFs according to the retention of initial PXRD patterns, loss of surface area, vibrational feature changes in FT-IR spectra, and mass changes after chemical treatments. Using this assessment protocol, some representative COFs featuring high chemical stabilities are summarized in Table 1 in reverse chronological order.

Following the appearance of first boroxine-linked COF-1 that is susceptible to water or protic solvents, a rapidly growing number of COFs with increasingly high chemical stability have been developed in recent years by virtue of the enormous structural tunability (Scheme 2). To safeguard COFs from structural destruction in abrasive conditions, three main approaches have been exploited to improve their chemical robustness: 1) decrease the reversibility of the covalent linkages of COFs via *de novo* synthesis, post-synthetic linkage conversion, or post-devitrification; 2) tailor the supramolecular noncovalent interactions including Brønsted-type interactions, hydrogen bonding, and interlayer stacking forces; 3) manipulate the inherent properties of linkers such as steric and hydrophobic natures by a rational selection of pre-designed linkers and post-synthetic modification.

2.1 Imparting COFs with high chemical robustness by strengthening the covalent linkage

The chemical stability of COFs is strongly related to the nature of the covalent linkages. Robust linkages, which reticulate organic units together to extended networks, remain inert to various stimulus chemicals and thus prevent the frameworks from structural collapse. There are two main approaches to imparting robust linkages in COFs, that is, *de novo* synthesis and post-synthetic modifications. Specifically, the *de novo* synthesis employs linking reactions that can yield robust linkages in one step or via reversible-irreversible cascades, while post-synthetic modifications refer to the post-synthetic linkage conversion in established COFs or post-devitrification of amorphous amide networks.

2.1.1 Robust linkage by a one-step reaction in *de novo* synthesis of COFs

Early examples of COFs, such as boroxine/boronate ester-linked and azodioxy-linked COFs,[21] suffer from hydrolytic instability. Such a problem stimulates researchers to develop new reactions for the construction of COFs, concurrently fulfilling the desire to both expand the scope and improve the intrinsic chemical stability of COFs. Since their birth in 2005, a growing number of linkages (~27 in total) have been explored in COFs synthesis (Figure 1).[22] Among these, some representative linkages such as imine,[23] azine,[24] triazine,[25] hydrazone,[26,27] squaraine,[28] imide,[29] phenazine,[28] β-ketoenamine,[30] olefin,[31] urea,[32] and aryl ether[33] hold great promise in the construction of chemically robust COFs largely due to their relatively strong bond strength over boron-based linkages. In this context, we mainly concentrate on the newly-developed linkages such as *β*-ketoenamine (via Michael addition-elimination), olefin, phenazine, and 1,4-dioxin, and summarize the most recent progress in the synthesis of robust COFs.

Since the first report in 2009,[34] imine-linked COFs have become the most extensively explored COFs to date.[35] However, these COFs are not efficient in facilitating π-delocalization due to the highly polarized imine bonds, and most COFs are still susceptible to hydrolysis, particularly in acidic medium. To this end, Perepichka and co-workers demonstrated in 2016 a novel and general synthetic approach toward crystalline COFs with improved π-delocalization and chemical stability using Michael addition-elimination reactions of *β*-ketoenols and arylamines in dioxane/mesitylene at 130 °C for 3 days .[36] The resulting *β*-ketoenamine-linked COFs displayed enhanced hydrolytic stability in 9 M aqueous HCl (aq.) and hot water (50 °C) over 7 days, which was attributed to the combined effects of locked *β*-ketoenamine linkage and intramolecular H-bonding (C=O···H-N). As a control, an imine-linked COF without H-bonding prepared by condensation between 1,3,5-triformyl benzene and *p*-phenylenediamine completely dissolved in 9 M HCl (aq.) within hours. Following the same strategy, Bojdys and co-workers reported a robust 2D *β*-ketoenamine-linked COFs by Michael addition-elimination reactions of (1,4-phenylene) bis(3-hydroxyprop-2-en-1-one) (PBHP) with 1,3,5-tris-(4-aminophenyl) triazine (TAPT). The synthesized COF (PBHP-TAPT) remained structurally intact after multiple cycles of exposure to HCl and NH_3 vapors.[37] More recently, Fang's group reported an ambient and eco-friendly pathway to construct robust *β*-ketoenamine-linked COFs (JUC COFs) via Michael addition-elimination reactions in an aqueous medium.[38] This novel approach features a high reaction rate (30 min), high yield (93%), and scalable preparation (5.0 g).

To further facilitate π-delocalization and improve chemical stability, developing 2D COFs with fully sp^2 carbon conjugated backbones is highly appealing. Since the first olefin-linked COFs prepared via Knoevenagel condensation in 2016,[31] COFs with highly conjugated olefin skeletons have triggered substantial attention due to their exceptional chemical stabilities,[39] intriguing magnetic coupling,[40] and superb photocatalytic activities.[41] A rapidly growing number of olefin-linked COFs (approximately 28 COFs) with varying topologies and functionalities have been constructed to date. In 2018, Jiang's group reported the designed synthesis of highly stable and luminescent sp^2 carbon-conjugated COFs by polycondensation of 1,3,6,8-tetrakis(4-formylphenyl) pyrene with 2,2′-(1,4-phenylene) diacetonitrile, 2,2′-(biphenyl-4,4′-diyl) diacetonitrile, or 2,2′-([1,1′:4′,1″-terphenyl]-4,4″-diyl) diacetonitrile (Figure 2).[42] The obtained sp^2c-COF, sp^2c-COF-2, and sp^2c-COF-3 displayed preserved crystallinity and porosity without apparent weight loss upon 7-day exposure to various solvents such as DMF, THF, MeOH and H_2O, concentrated 12 M HCl (aq.) and 14 M NaOH (aq.). Strikingly, the sp^2 c-COFs are stable upon 1-year exposure to air at ambient temperature with intact crystallinity and porosity, whereas the imine-linked COF counterpart cannot retain its crystallinity under identical conditions. Nevertheless, the strong electron-withdrawing nitrile (-CN) groups appended to the olefin (C=C) bond make the cyanovinylene linkage reversible while compromising the stability of COFs.[39,43] In 2019, Yaghi's group firstly reported an unsubstituted olefin-linked COF (COF-701) through a Brønsted acid-catalyzed Aldol condensation of 2,4,6-trimethyl-1,3,5-triazine and 4,4'-biphenyldicarbaldehyde in a mixture of mesitylene/1,4-dioxane/acetonitrile at 150 °C for 3 days.[44] The unsubstituted olefin linkage endows COF-701 with exceptional chemical stability toward strong acid and base (12.1 M aqueous

HCl, saturated aqueous KOH, and saturated methanolic KOH at room temperature for 24 hours), organolithium reagents (1 M *n*-BuLi in THF/hexanes and 0.8 M MeLi in THF/Et_2O at -78 °C), and Lewis acid ($BF_3 \cdot OEt_2$). The olefin-linked COFs have garnered tremendous attention as a robust and tailorable platform for various applications including photocatalysis,[41,45-47] supercapacitors,[48] and environmental remediation.[49]

The phenazine linkage has gained increasing popularity due to its fused planar structure and high stability to afford fully annulated robust COFs. In 2013, Jiang's group reported the first phenazine-linked COFs (CS-COF) by the acetic acid-catalyzed condensation of triphenylene hexamine and *tert*-butylpyrenetetraone monomers in ethylene glycol at 120 °C for 3 days. CS-COF exhibited superb chemical stability, extended π-delocalization, and capability to host guest molecules and hole mobility.[28] In 2019, Mirica and co-workers developed a robust and intrinsically conductive phthalocyanine-based COF (COF-DC-8) through the aromatic annulation of 2,3,9,10,16,17,23,24-octa-aminophthalocyanine nickel (II) with pyrene-4,5,9,10-tetraone, catalyzed by sulfuric acid in a 1:1 dimethylacetamide (DMAc)/o-dichlorobenzene mixed solvent at 202 °C for 10 days. Most recently, Jiang's group reported a topologically identical phenazine-linked metallophthalocyanine CoPc-PDQ-COF by the condensation of 2,3,9,10,16,17,23,24-octakis(amino) phthalocyanine cobalt (II) with 4,5,9,10-pyrenediquinone in the presence of acetic acid (AcOH)/DMAc/ethylene glycol at 200 °C for 7 days.[50] Due to the robust nature of phenazine, CoPc-COF showed strikingly high chemical stability in various organic solvents, 12 M HCl (aq.), and 14 M NaOH (aq.) for as long as 40 days. Other attempts using similar condensation reactions include the synthesis of phenazine-linked COFs by covalently stitching 1,2,4,5-benzenetetramine tetrahydrochloride and hexaketocyclohexane octahydrate.[51] Conventional acid-mediated solvothermal synthesis typically resulted in amorphous polymers.[52,53] To tackle this challenge, Liu and co-workers recently reported the unusual dynamic characteristics of the C=N bonds in the pyrazine ring promoted under basic aqueous conditions at 120 °C for 3 days,[54] which enabled the successful synthesis of porous graphitic frameworks (PGF-1) with fully annulated aromatic skeletons and periodic pores (Figure 3A). The crystallinity of PGF-1 was verified by PXRD analysis in conjugation with high-resolution transmission electron microscopy (HRTEM). The honeycomb microporous structure of PGF-1 was clearly visualized along the [001] plane with a uniform pore size of 1.2 ± 0.1 nm, which was consistent with the simulated model (Figure 3B).

In 2019, Yaghi and co-workers introduced nucleophilic aromatic substitution (S_NAr) into the realm of COFs (Figure 3),[33] whereby two unprecedented dioxin-linked COFs, COF-316 and COF-318, were prepared by the reactions of 2,3,6,7,10,11-hexahydroxy triphenylene with tetrafluorophthalonitrile and 2,3,5,6-tetrafluoro-4-pyridinecarbonitrile in the presence of catalytic bases at 120 °C for 3 days, respectively. The COFs exhibited exceptionally high chemical stability after treatment in concentrated HCl and NaOH solutions with full retention of crystallinity. Using the identical strategy, Fang's group reported a series of polyarylether-based COFs (PAE-COFs, Figure 4) through S_NAr reactions between ortho-difluoro benzene and catechol building units.[55] The PAE-COFs displayed high crystallinity, porosity, and outstanding chemical stability. PAE-COFs retained their pristine crystallinity after exposure to a wide array of extreme conditions such as HCl (12 M), concentrated H_2SO_4 (18 M), NaOH (14 M), MeONa (5 M in MeOH), chromic acid solution (0.1 M $K_2Cr_2O_7$ in concentrated H_2SO_4) and $LiAlH_4$ (2.4 M in THF), outperforming a series of other known chemically stable COFs, prototypical metal-organic frameworks (MOFs) (UiO-66, ZIF-8, HKUST-140, and MOF-541) and zeolites (commercial silicalite-1, X, Y, and 4A). This strategy opens up a novel pathway for the design and construction of chemically robust COFs through S_NAr reactions. It should be noted that while such S_NAr reactions are traditionally regarded as irreversible, aryl ethers linkages are known to display reversible bond characters,[56,57] thus a dynamic reaction mechanism cannot be excluded and is worth more careful investigation.

2.1.2 Robust linkage via a reversible-irreversible cascade

The synthesis of COFs with robust linkages can be realized via a cascade reaction that combines reversible linkage formation with a subsequent *in situ* irreversible transformation (e.g., tautomerization and cyclization). This stepwise approach is highly appealing because it capitalizes on two sequential reactions to realize both crystallinity and stability, with the first reaction to provide the thermodynamic reversibility and the second to afford the kinetically stable product.

For instance, Banerjee and co-workers firstly developed a methodology of combined reversible and irreversible transformations to synthesize chemically stable COFs in 2012.[30] The two β-ketoenamine-linked COFs (TpPa-1 and TpPa-2) were constructed by the reactions of 1,3,5-triformyl phloroglucinol (Tp) with *p*-phenylenediamine (Pa-1) and 2,5-dimethyl-*p*-phenylenediamine (Pa-2) in the presence of 3 M AcOH in 1:1 mesitylene/dioxane solvent at 120 °C for 3 days, respectively (Figure 5). The enol-imine bonds underwent irreversible proton tautomerization to

yield a more stable keto-enamine form, which conferred TpPa-1 and TpPa-2 with superb chemical stability in boiling water, strongly acidic (9 M HCl) and basic (9 M NaOH) solutions. With this enol-to-keto tautomerization strategy, a large number of chemically robust β-ketoenamine-linked COFs (approximately 40 COFs in total) have been constructed and implemented in diverse applications such as catalysis,[58] radionuclide sequestration,[59] energy storage,[60] and proton conduction.[61]

Triazine is another robust linkage that endows COFs with high chemical stability and rich nitrogen content. In 2008, Thomas and co-workers reported the first covalent triazine frameworks (CTFs) with triazine linkages using ionothermal synthesis in molten $ZnCl_2$ at 450 °C.[25] However, CTFs from early attempts were mostly amorphous or semi-crystalline. High temperature and metal catalysts required for the isothermal synthesis present additional hurdles for the broad utility of CTFs. To this end, a handful of new synthetic strategies have been developed to prepare crystalline CTFs at milder conditions, such as phosphorus pentoxide-mediated synthesis, amidine-based polycondensation, and superacid-catalyzed synthesis.[62,63] In 2017, Tan's group developed a new cascade Schiff-base-Michael addition reaction to prepare four crystalline CTFs (CTF-HUST 1-4) at relatively low temperatures (120 °C). The CTFs were constructed via condensations between the aldehyde and amidine dihydrochloride using cesium carbonate as the catalyst and DMSO/H_2O as the solvent (Figure 6).[64] To further improve the crystallinity of CTFs, Tan's group later developed an *in-situ* oxidation strategy using aryl alcohols as monomers that were gradually oxidized to aldehydes in DMSO in the presence of air and cesium carbonate.[65] Using this strategy, a series of crystalline CTFs (CTF-HUST-Cs) were prepared in a round-bottom flask. Enhanced crystallinity of CTFs at mild conditions was also achieved by controlling crystal nucleation and growth using a fine-tuned feeding rate of the aldehyde monomer.[63] In recent subsequent work, they demonstrated a base-assisted route for the synthesis of crystalline CTF (CTF-HUST-A1) using a new benzylamine-based monomer in the presence of DMSO and strong base.[66] CTF-HUST-A1 possesses high crystallinity and hydrophilic property, which leads to high activity in photocatalytic hydrogen evolution. These robust crystalline CTFs prepared by mild synthetic methodologies open up new opportunities in a broad array of applications.

In 2018, Wang and co-workers deployed another reversible-irreversible cascade reaction to prepare ultra-stable benzoxazole-linked COFs (LZU-190–192) (Figure 7).[67] The benzoxazole-linked COFs were synthesized by the condensation of 2,5-diamino-1,4-benzenediol dihydrochloride with various aryl aldehydes using 1:1 *N*-methyl-2-pyrrolidone (NMP) and mesitylene as the solvent, benzimidazole as the additive, and 185 °C as the reaction temperature for 5 days. The formation of benzoxazole rings proceeded through a three-step transformation: (1) initial formation of phenolic imine-linked intermediates, (2) ring closure and formation of benzoxazoline intermediates, and finally (3) dehydrogenation of benzoxazoline intermediates to yield benzoxazole rings. LZU-190 possessed substantially higher crystallinity than that of an identical COF (BBO-COF-1) first obtained by a one-pot NaCN-mediated solvothermal synthesis reported by McGrier's group in 2016.[68] The robust benzoxazole linkages endowed the COFs with high chemical resistance toward strong acid (9 M HCl, trifluoroacetic acid) and strong base (9 M NaOH) for 3 days. In contrast, the imine-linked COF-LZU-1 dissolved under these conditions, underscoring the superior stability of benzoxazole over conventional imine linkage. Later, the same group constructed a series of robust imidazole-linked COFs (LZU-501 and LZU-506) via a Debus-Radziszewski multicomponent reaction, which involved the covalent assemblies among diketone, ammonia, and aldehyde in a 1:4 dioxane/mesitylene mixed solvent at 150 °C for 5 days.[69] The imidazole-linked COFs maintained their crystallinities upon 3-day treatment in solvents such as DMF and H_2O, 9 M NaOH (aq.) and 9 M HCl (aq.). Another version of imidazole-linked COF was also readily constructed by a cascade polyphosphoric acid-mediated condensation between 1,3,6,8-tetrakis(*p*-benzoic acid) pyrene and 1,2,4,5-benzenetetramine tetrahydrochloride.[70] Due to the robust linkage and highly periodic skeletons, the imidazole-linked 2D COF exhibited a record-high proton conductivity (3.2×10^{-2} S cm^{-1}) (at 95% relative humidity and 95 °C). More recently, thiazole linkage was introduced in 2D COFs by a cascade reaction that involved sequential imine and thiazole formation.[71] Gu and co-workers synthesized two stable benzothiazole-linked COFs (PG-BBT and BZ-BBT) by one-pot reactions of 2,5-diamino-1,4-benzenedithiol dihydrochloride with aryl aldehydes catalyzed by 3 M AcOH in dioxane/mesitylene at 120 °C for 3 days. The benzothiazole-linked COFs retained their inherent properties after 7-day exposures to boiling water, 3 M HCl (aq.), and 3 M KOH (aq.). However, this strategy requires the use of the *ortho*-aminothiophenol monomer that has limited availability, thus hampering the scope of this methodology. To circumvent such issues, Wang *et al.* prepared five stable thiazole-linked COFs (TZ-COFs) through a facile three-component reaction involving aryl aldehydes, amines and elemental sulfur in the presence of acetic acid and DMSO at 120 °C for 3 days.[72] The formation of thiazole linkage was readily obtained by a cascade of imine condensation, C-H functionalization, and oxidative annulation. The robust thiazole

linkages conferred TZ-COFs strong chemical stability in 12.5 M HCl (aq.) at 50 °C, 12 M KOH (aq.), 1 M CH_3ONa (aq.), and 1 M $NaBH_4$ (aq.) at room temperature for 2 days.

Most recently, Dong's group developed a new cascade reaction that combined imine condensation and cycloadditions (Strecker or Povarov reactions) to prepare twelve highly stable α-aminonitrile- and quinoline-linked COFs.[73] In essence, the three-component, one-pot Povarov reaction among 1,3,5-tri(4-aminophenyl) benzene, 2,5-dimethoxy terephthalaldehyde, and styrene was carried out in the presence of catalytic AcOH and $BF_3{\cdot}OEt_2$ at 120 °C for 3 days to afford COFs with irreversible quinoline linkages. In comparison to the imine-linked and α-aminonitrile-linked COFs, quinoline-linked COFs displayed much higher chemical stability. In a similar fashion, the one-pot cascade imine condensation-cycloaddition reactions were employed by Zhang's group for the synthesis of ultrastable tetrahydroquinoline-linked COFs (QH-COFs), which were constructed by the reaction of 3,5-tris(p-formylphenyl)benzene with benzidine in the presence of ethyl vinyl ether using a mixture of $Sc(OTf)_3$ and $Yb(OTf)_3$ as catalysts and 1,2-dichlorobenzene/*n*-butyl alcohol as solvent at 120 °C for 3 days.[74] QH-COF-1 showed ultrahigh chemical stability and remained intact after a 3-day treatment in trifluoroacetic acid, 12 M HCl (aq.), 14 M NaOH (aq.), and even concentrated H_2SO_4 (98%). In contrast, the imine-linked COF (COF-1) was digested completely in strong acidic or basic solutions. Compared with previous cascade reactions that have a limited scope, this sophisticated cascade Schiff-base-cycloaddition represents a promising route for the construction of robust COFs with a broader scope.

In deviation of the predominant cascade Schiff-base-cycloadditions, Gu's group recently reported two benzofuran-linked COFs (GS-COF-1 and GS-COF-2) through a one-pot cascade reaction that involves cyanovinylene formation, cyanide migration, ring-closure, and oxidation reactions.[75] Highly crystalline and porous GS-COFs were prepared via reactions between 2,5-dihydroxyterephthalaldehyde or 1,3,5-triformyl phloroglucinol and 2,2',2''-(benzene-1,3,5-triyl) triacetonitrile or 2,2'-(1,4-phenylene) diacetonitrile in the presence of potassium tert-butoxide and oxygen at 110 °C for 6 days. Due to the irreversibility of benzofuran linkages, CS-COFs retained their inherent crystallinity and porosity upon a 3 day-treatment in concentrated HCl (aq.) and NaOH (aq.) at room temperature. Moreover, the exceptional stability allowed the successful post-synthetic modification of cyano groups into carboxylic acids under harsh conditions (H_2SO_4 and AcOH aqueous solution at 105 °C for 2 days).

2.1.3 Robust linkage via post-synthetic linkage conversion

Albeit the significant progress accomplished, imparting robust linkage by *de novo* synthesis still has inherent limitations, such as limited scope and crystallization problems encountered in COFs synthesis, which involves tedious conditions screening. Post-synthetic modification (PSM), which allows the preparation of topologically identical but functionally diverse frameworks through chemical modifications of pre-formed COFs, offers enormous functional and structural flexibility in new functional materials development.[76,77] PSM renders elegant control over both the pendant functional groups in COFs and the covalent linkages. The post-synthetic linkage conversion paves the way to access COFs linkages that are difficult or impossible to access *de novo* while bypassing the usual crystallization problems in COFs synthesis. Imines, the most explored COF linkages, have served as the only platform thus far for the exploration of post-synthetic linkage conversion (Figure 8), except one recent report on the transformation of olefin-linked 2D COF to cyclobutane-linked 3D COF via [2+2] cycloaddition of olefin linkages.[78]

The first post-synthetic linkage conversion in COFs was reported by Yaghi's group in 2016.[79] They derived two amide-linked COFs that are difficult to access *de novo* by mild Pinnick-type oxidation of the imine-linked COFs using sodium chlorite as the oxidant and AcOH as the catalyst at room temperature for 2 days (Figure 8A). The amide-linked COFs retained crystallinity and porosity after the linkage conversion. Furthermore, the amide COFs remained intact in 12 M HCl (aq.) and 1 M NaOH (aq.) for 1 day while the pristine imine COFs were rendered amorphous. Such vastly different stability corroborated with the successful conversion from reversible imines to irreversible amides. In 2018, Lotsch's group demonstrated a topochemical conversion of a 2D imine-linked COF (TTI-COF) into a thiazole-linked COF using a post-synthetic locking strategy (Figure 8B).[80] The imine-linked TTI-COF was first infiltrated with molten sulfur at 155 °C. Subsequently, the temperature was raised to 350 °C and elemental sulfur oxidized the imine to a thioamide, which oxidatively cyclized to form a thiazole unit. Upon the imine-to-thiazole transformation, the resultant thiazole-linked TTT-COF displayed more pronounced stability against harsh conditions than the imine-linked TTI-COF precursors, such as alkaline conditions (12 M KOH and 1 M NaOH at 50 °C) and reducing agents (1 M hydrazine and 1 M $NaBH_4$). Moreover, the robust thiazole linkage conferred TTI-COF with high electron beam stability, facilitating an in-depth TEM study to visualize the defect sites and grain boundaries of COFs.

In addition to the sulfur-assisted thiazole formation at high temperature, oxazole and thiazole linkages are achievable in COFs through a milder PSM approach. In 2018, Yaghi and co-workers developed a series of highly

stable oxazole and thiazole-linked COFs by linker substitution with subsequent oxidative cyclization of existing imine-linked COFs.[81] Specifically, they incorporated desired functionalized linkers into a well-studied imine-linked COF (ILCOF-1) via post-synthetic linker exchange, followed by oxidative cyclization to convert imine into oxazole and thiazole under O_2 at 85 °C for 1 day (Figure 8C). Due to the irreversibility of the azole linkages relative to the imine, the azole-linked COFs retained structural integrity under various harsh conditions including strongly basic (10 M NaOH) and acidic (18 M H_2SO_4, 14.8 M H_3PO_4, 12.1 M HCl, and 9 M H_2SO_4 in DMSO) solutions for one day while pristine ILCOF-1 treated with H_2SO_4 lost its original phase. Analogously, benzoxazole-linked COFs were derived from the conversion of an imine-linked COF via post-oxidative cyclization by Baek's group in 2019 (Figure 8E).[83] The succinct and efficient post-treatment transformed an unstable COF into a robust COF with irreversible linkage using 2,3-dichloro-5,6-dicyano-1,4-benzoquinone (DDQ) as the oxidant and dry CH_2Cl_2 as the solvent at room temperature for 3 days, which displayed dramatically improved chemical stability and high crystallinity. The benzoxazole-linked COF retained its inherent properties after exposure to boiling water, 12 M HCl (aq.), and 10 M NaOH (aq.) for 3 days. In stark contrast, the imine-linked COF showed great loss of crystallinity and porosity after identical treatments. The robust benzoxazole-linked COFs showed full retention of crystallinity and porosity upon further treatments with methanesulfonic acid, 1 M H_2SO_4 (aq.), and 1 M $NaBH_4$ (aq.), which underscored the successful linkage transformation and its high stability.

To achieve dual goals of enhanced robustness and π-delocalization in COFs, Liu and co-workers developed in 2018 a facile strategy that transformed imine-linked COFs into ultrastable crystalline porous aromatic frameworks, MF-1, by kinetically locking the reversible imine linkages via an aza-Diels-Alder cycloaddition reaction (Figure 9A).[86] After reacting with various phenylacetylene derivatives using $BF_3{\cdot}OEt_2$ as the catalyst and chloranil as the oxidant at 110 °C for 3 days, the imine-linked COF was converted into corresponding quinoline-linked COFs in a yield of ~30%. The resultant quinoline-linked COFs not only retained crystallinity and porosity but also displayed significantly enhanced chemical stability in comparison to their imine COF precursors. These COFs (MF-1a) are among the most robust COFs that can withstand strong acidic (boiling 12 M HCl and triflic acid), basic (14 M NaOH), reductive ($NaBH_4$) and oxidative ($KMnO_4$) treatment (Figure 9B), and prolonged exposure such as immersion in concentrated HCl solution at room temperature for two months. In addition to the pronounced chemical stability, this protocol also allowed for fine-tuning of the pore surface to realize pre-designed surface wettability (Figure 9C), by the chemical diversity of the cycloaddition reaction and structural tunability of COFs.

Most recently, Zhang and co-workers synthesized two fused-aromatic thieno [3,2-c] pyridine-linked COFs (T-COF-2 and B-COF-2) by a post-synthetic Pictet-Spengler cyclization of imine-linked COFs (Figure 8F).[84] Two imine-linked COFs bearing thiophene groups adjacent to imine centers were synthesized at first. A post-cyclization (Pictet–Spengler reaction) between the *β*-carbon of thiophene and the carbon of imine linkage in the presence of O_2 and catalytic trifluoracetic acid at 100 °C for 2 days gave rise to thieno[3,2-c]pyridine linkages. Remarkably, the irreversible linkage imparted thieno [3,2-c] pyridine-linked COFs with high chemical resistance toward 12 HCl (aq.) and 12 M NaOH (aq.) at 50 °C.

2.1.4 Robust linkage by post-devitrification of amorphous networks

Amide bonds are highly stable and irreversible under practical conventional conditions, which preclude the error-checking and defect-repairing during COFs synthesis. Therefore, it is extremely challenging to directly synthesize amide-linked COFs *de novo*. As was mentioned before, Yaghi's group tackled such a challenge by deriving amide-linked COFs via post-synthetic oxidation of pre-formed imine-linked COFs. Most recently, Yan's group synthesized an amide-linked COF (JNU-1) by a post-synthetic linker exchange of 4,4'-biphenyldicarboxaldehyde in an imine-linked COF with terephthaloyl chloride.[87] Taking a different approach, Rosseinsk's group prepared two crystalline covalent amide frameworks (CAFs) with 2D and 3D topologies by post-devitrification of amorphous polyamides under high-temperature and high-pressure reaction conditions (Figure 10).[88] This transformation was realized by charging amorphous polyamide precursors in a Parr pressure reactor with water, which was sealed and heated at 250 °C for 3 days. The hydrolytic stability of crystalline CAF-1 and CAF-2 was assessed by immersing them in boiling water, 1 M boiling HCl (aq.) and NaOH (aq.) for 1 day, or in 12 M HCl (aq.) and 14 M NaOH (aq.) at ambient temperature for 7 days. Both CAF-1 and CAF-2 remained intact under these conditions. This example represents the first report that an amorphous organic material could be readily converted into its crystalline counterpart in high-temperature water[89] and serves as a proof-of-principle that post-devitrification is a viable approach to ultrastable COFs bearing linkages (e.g., amide) that are irreversible under conventional conditions.

2.2 Improving chemical stability through supramolecular noncovalent interactions

Asides from altering the bond reversibility of covalent linkage, the supramolecular noncovalent interactions (e.g., hydrogen bonding and interlayer stacking forces) are also essential to the chemical stability of COFs. A variety of studies have been performed to prepare chemically robust COFs through tailoring supramolecular noncovalent interactions.

2.2.1 Brønsted-type interactions in boroxine-linked COF

As the first example of COFs reported in 2005, boroxine/boronate ester-linked COFs possess intrinsic hydrolytic instability that greatly hampers their potential applications.[90] To address the stability issue, Calabro and co-workers used pyridine to protect the boronate ester linkages of COF-5 from hydrolytic degradation.[91] However, this approach has limited scope and only led to slightly enhanced stability. In 2015, Du and co-workers attempted to insert Si-O bonds into boroxine-linked COF-1 and deliberately created Brønsted acid defect sites,[92] followed by the addition of an alkylamine to produce a combination of Lewis and Brønsted interactions, which were proved effective in stabilizing boron-based COFs (COF-5 and COF-10). The addition of (3-aminopropyl) triethoxysilane (APTES) and alkylamine to the COF-1 yielded a stable composite (APTES-COF-1) due to Brønsted type interactions. APTES-COF-1 remained air-stable after 4 months whereas the conventional COF-1 fully decomposed within hours, indicating a dramatic improvement in stability. Thanks to the enhanced hydrostability, Xi and co-workers employed APTES-COF-1 to prepare a water-dispersible polymer-COF hybrid (PEG-CCM@APTES-COF-1) from the assembly of COF with polyethylene-glycol-modified monofunctional curcumin derivatives, which was utilized as smart carriers for drug delivery with superb anticancer therapeutic efficiency.[93] It should be noted that despite the enhanced hydrostability by Brønsted-type interactions, the chemical stability of boron-based COF is still far from satisfactory due to the intrinsically labile linkage.

2.2.2 Inter- and Intra-molecular hydrogen-bonding

Hydrogen-bonding (H-bonding) interactions in imine-linked COFs can suppress the torsion of the edges and lock the 2D sheets to align in one plane, hence improving the π-π stacking between the adjacent COF layers and exerting a positive effect on their chemical stability and crystallinity.[94] Using this principle, Banerjee and co-workers rationally introduced intramolecular and intermolecular H-bonding in 2D layered frameworks to develop COFs with exceptional chemical robustness.

In 2013, Banerjee and co-workers introduced hydroxy (-OH) functionalities adjacent to the imine centers in the COF DhaTph, which was synthesized by the Schiff-base reaction of 2,5-dihydroxyterephthalaldehyde (Dha) with 5,10,15,20-tetrakis(4-aminophenyl)-21H,23H-porphine (Tph).[95] DhaTph COF showed high chemical stability and retained its crystallinity in boiling water or 3 M HCl (aq.) over 7 days. To validate the essential role of intramolecular H-bonding [–O-H···N=C], they prepared a methoxy-substituted COF without intramolecular H-bonds and found the COF showed lower chemical stability and crystallinity. They later reported in 2015 the synthesis of a chemically robust hollow spherical COF (DhaTab) by the Schiff-base reactions of Dha and 1,3,5-tris(4-aminophenyl) benzene (Tab).[96] The strong intramolecular H-bonding conferred DthTab COF with high chemical stability that sustained 7-day exposure to water, 3 M HCl (aq.) and phosphate buffer at pH 7.4.

Apart from intramolecular H-bonding, intermolecular H-bonding can also be utilized to improve the chemical stability of imine-linked COFs. The same group developed in 2018 a series of ultrastable 2D COFs by incorporating methoxy functionalities in the 2,4,6-trimethoxy-1,3,5-benzenetricarbaldehyde (Figure 11A).[97] These COFs displayed strikingly high chemical stability in concentrated 18 M H_2SO_4, 12 M HCl (aq.), and 9 M NaOH (aq.) for several days. This work is amongst the first report showcasing imine-linked COFs with exceptional chemical stability in such drastic media. With the aid of theoretical calculations, they postulate that the strong interlayer C-H···N H-bonding between the methoxy of one layer with the imine (C=N) nitrogen in the adjacent layer (Figure 11B) accounts for the exceptional stability by providing a steric and hydrophobic environment near the imine centers to safeguard them from hydrolysis in harsh conditions.

2.2.3 Reducing interlayer electrostatic repulsion

Besides H-bonding, the interlayer charge repulsion between COFs layers is central to the stability as well as crystallinity. In imine-linked COFs, the C=N bond is polarized to produce partially positively charged carbon and negatively charged nitrogen, resulting in electrostatic repulsion in between fully eclipsed COF layers. To alleviate the interlayer repulsion, Jiang and co-workers incorporated electron-donating methoxy groups into the pore walls to afford a highly chemically robust COF, TPB-DMTP-COF (Figure 12A), which was prepared by the condensation between 1,3,5-tri-(4-aminophenyl) benzene (TAPB) and dimethoxy terephthaldehyde (DMTP).[98] The introduction of electron-donating methoxy groups to the positively charged edges reduces the interlayer electrostatic repulsion

and stabilizes the COF stacking layers, resulting in an overall enhancement of the chemical stability and crystallinity. TPB-DMTP-COF preserved its crystallinity and porosity after treatments of various organic solvents, boiling water, aqueous strong acid (12 M HCl) and base (14 M NaOH) for 7 days. A set of control experiments has been conducted to validate the essential role of methoxy groups in stabilizing COF. TPB-TP-COF, the homolog to TPB-DMTP-COF but without methoxy groups, and TPB-DHTP-COF (DHTP, dihydroxy terephthaldehyde) with -OH functionalities that permit intramolecular H-bonding, both exhibited lower chemical stabilities, revealing the pivotal stabilization effects of methoxy groups. Such extraordinary chemical stability marked TPB-DMTP-COF as the most chemically stable COF at the time it was reported. Following the analogous strategy, the same group recently incorporated another electron-donating methyl groups into the phenyl linkers to prepare a highly stable TPB-DMeTP-COF (Figure 12B), which was synthesized by the condensation of TAPB and dimethyl terephthaldehyde (DMeTP).[99] TPB-DMeTP-COF was chemically robust to retain intact in CH_3CN, THF, boiling water, H_3PO_4 (0.7 M in THF), 12 M HCl (aq.), and 14 M NaOH (aq.) for 7 days. Thanks to the remarkable chemical robustness, neat H_3PO_4 was encapsulated into TPB-DMeTP-COF, and the obtained hybrid materials allowed proton super flow across the 1D channels.

2.3 Improving chemical stability by manipulating intrinsic properties of linkers

The primary concern for COF chemical stability has been largely related to water. By tuning the steric and hydrophobic properties of linkers, one can mitigate the hydrostability of COFs by kinetically blocking and repelling water from the linkers.

2.3.1 Steric tuning

Using a multivariate approach, Cui and co-workers showcased the first systematic synthetic control of both the layer stacking modes and chemical stability of 2D COFs by manipulating interlayer steric hindrance.[100] They developed a family of two-, three-, and four-component 2D imine-linked COFs adopting AA, AB, or ABC stacking modes, by co-condensations of triamines with/without alkyl substituents (ethyl and isopropyl) and di- or tri-aldehydes. COFs with a higher density of alkyl groups adopted AB or ABC stacking, while a lower number of alkyl substituents led to COFs in AA stacking. The installed alkyl groups modulated the stacking mode and chemical stability of 2D COFs by maximizing the crystal stacking energy and protecting hydrolytically vulnerable backbones via kinetic blocking water molecules from accessing the reaction sites. The COF bearing a high number of isopropyl groups can retain its inherent properties in a boiling 20 M NaOH (aq.) and 0.1 M HCl (aq.) for 7 days.

2.3.2 Hydrophobicity engineering

Engineering the wettability of solid materials has summoned tremendous attention due to their potential for diverse applications. Imparting hydrophobicity on hydrolytically vulnerable materials could safeguard them against hydrolysis. For instance, coating a protective hydrophobic layer on the surface of MOFs has been proven as an effective means for improving hydrolytic stability with the retention of their intrinsic properties.[101] Despite the nascent stage, engineering surface hydrophobicity of COFs by employing hydrophobic monomer units or post-synthetically attaching hydrophobic moieties onto the established COFs has been proven as a viable means to protect hydrolytically susceptible COFs from hydrolysis.

In 2019, Chen and co-workers developed a two-in-one strategy for the *de novo* synthesis of a highly stable imine-linked COF (Py-COF) through a self-condensation of 1,6-bis(4-formylphenyl)-3,8-bis(4-aminophenyl)pyrene that possesses both formyl and amino groups.[102] Py-COF showed excellent chemical stability in boiling water, 12 M NaOH (aq.), and 12 M HCl (aq.) for 3 days, which was presumably attributed to the high hydrophobicity of COF. Later, the same group reported another imine-linked BBO-COF by the self-condensation of a new A2B2 monomer, 4,4′-(2,6-bis(4-aminophenyl)benzo[1,2-d:4,5-d′]bis-(oxazole)-4,8-diyl) dibenzaldehyde.[103] BBO-COF also showed high chemical stability after 7-day treatments with boiling water, trifluoroacetic acid, 12 M NaOH (aq.) and 12 M HCl (aq.). Most recently, Horike's group prepared a series of superhydrophobic hydrazone-linked 2D COFs (COF-F6, COF-F8, and COF-F10) via condensations of 1,3,5-triformylbenzene and three perfluoroalkyl-functionalized hydrazide monomers.[104] The superhydrophobicity allowed COF-F6 to preserve its crystallinity and porosity upon 1 day-treatment in HCl (38%), and HNO_3 (65%) and H_3PO_4 (85%) at room temperature. In contrast, the non-fluoroalkyl COF counterpart lost its crystallinity. Due to the ultra-stability towards acid, COF-F6 was employed as robust support to host H_3PO_4 for rapid and long-term proton conduction under a wide range of temperatures. In addition to 2D COFs with tailor-made hydrophobic surfaces, Fang's group reported a strategy to impart hydrolytic stability of 3D COFs by incorporating hydrophobic isopropyl groups onto the 3D skeletons (JLU-530 and JLU-531),[105] which were prepared by the condensation of tetraphenyl methane containing 2,6-diisopropyl aniline and terephthalaldehyde or 4,4′-biphenyldicarboxaldehyde, respectively. The hydrophobic isopropyl groups imparted the

resultant 3D COFs with exceptional hydrolytic stability in a series of harsh environments including strong acids (3 M HCl and 3 M H_2SO_4 for one week), 20 M NaOH (aq.) for one week and boiling water for one month.

Unlike the *de novo* synthesis above, Ma's group demonstrated a post-synthetic modification approach to fabricate superhydrophobic COF (COF-VF). They first synthesized an imine-linked COF with terminal vinyl moieties (COF-V), followed by grafting 1*H*,1*H*,2*H*,2*H*-perfluorodecanesulfide onto COFs via a thiol-ene coupling reaction (Figure 13).[106] Upon the attachment of perfluoroalkyl groups, the hydrophobicity of COF increased dramatically with a water contact angle of ~167°. To validate the chemical shielding effect from the superhydrophobic surface, COF-VF was treated with boiling water, 12 M HCl (aq.) and 14 M NaOH (aq.) at room temperature for 7 days and still maintained its crystallinity and porosity. Furthermore, COF-VF exposed to 100% relative humidity under HCl or NH_3 atmosphere over 48 hours did not show any noticeable change in crystallinity. In sharp contrast, COF-V decomposed in 2 M HCl (aq.) or HCl gas in 12 hours. These results clearly suggest that hydrophobic modifications of the COFs surface can dramatically enhance their chemical stability.

3. Properties and Applications

To unleash the full potential of COFs in widespread applications, stability is a prerequisite to preserve the pristine properties of COFs in complex chemical environments. In addition to common stability requirements for COFs towards solvents (e.g., H_2O, DMF, DMSO), corrosives (acid, base), and air, there are specific considerations in applications ranging from heterogeneous catalysis, water remediation, chiral separation, corrosive gas sensing, and lithium-ion batteries. For instance, redox stability is essential for applications such as photocatalysis, electrocatalysis and energy storage. Besides, photostability under light irradiation is important for COFs to function as viable photocatalysts. Chemical stability towards nucleophiles and electrophiles needs to be satisfied for applications of COFs in conventional heterogeneous catalysis. For environmental remediation, COFs have to bear high stability towards the aqueous medium of varying pH and ion strength. These considerations inspire the recent advances in synthetic COF chemistry, as illustrated in the following examples.

3.1 Heterogeneous catalysis

COFs have emerged as an intriguing platform for heterogeneous catalysis due to its unique structural features, such as the spatial isolation and uniform distribution of multiple catalytic sites, and highly porous and periodic channels that ensure facile access of substrates to the catalytic sites.[107] The limited chemical stability of the COF catalyst is, however, detrimental for achieving sustained and efficient performance, particularly the catalytic processes involving abrasive chemicals and varying pH ranges. As such, the devoted effort towards the synthesis of stable COFs has greatly advanced their applications for heterogeneous catalysis.

In 2018, Deng's group synthesized robust amine-linked COFs with 2D and 3D topologies by the reduction of imine-linked pristine COFs with sodium borohydride in methanol at low temperature for a few hours.[85] The quantitative reduction of imines was verified by FT-IR and (^{13}C and ^{15}N) cross-polarization magic angle spinning solid-state NMR spectroscopies. The resulting amine-linked COFs showed high crystallinity and exhibited excellent chemical stability in strongly acidic (6 M HCl) and basic (6 M NaOH) solutions. In contrast, the pristine imine-linked COF was completely digested in HCl (aq.) and partially degraded in NaOH (aq.) Moreover, the amine-linked COFs exhibited significantly enhanced selectivity and Faradaic efficiency in the electrochemical reduction of CO_2 to CO using a COF-coated silver electrode in comparison to the imine COF precursor (Figure 14). Carbamate was identified to be the key intermediate in the efficient electrocatalytic CO_2 reduction process. The improved performance of CO_2 reduction over hydrogen evolution reaction was attributed to the enhanced chemical stability and chemisorptive concentration of CO_2 in the amine-linked COF.

In addition to electrocatalysis, robust COFs have emerged as efficient metal-free catalysts in visible-light photocatalysis due to their enormous structural turnability and chemical stability.[108,109] For high-performance photocatalysts, the long-term stability (e.g., photostability and chemical stability) under light irradiation and operating conditions are foundational for their practical applications. In 2018, Wang's group employed the cascade reaction strategy to prepare a series of ultrastable benzoxazole-linked COFs (LZU-190, LZU-191, and LZU-192) with exceptional photostability under visible light irradiation, and chemical stability in strong acids and bases compared to imine COFs. Besides stability, LZU COFs displayed enhanced visible-light absorption and were employed as catalysts for visible-light-induced oxidative hydroxylation of arylboronic acids to phenols. The benzoxazole-linked COFs exhibited high activity and outstanding recyclability even after twenty cycles of reactions. As a comparison, the imine-linked COF-1 decomposed under identical experimental conditions, underscoring the vital role of chemical stability in photocatalysis. In another example, Wang's group synthesized a 2D porphyrin-based sp^2 carbon-conjugated COF (Por-sp^2c-COF) by Knoevenagel condensation of 5,10,15,20-tetrakis(4-benzaldehyde) porphyrin and 1,4-phenylenediacetonitrile.[110] Thanks to the robust olefin linkages, Por-sp^2c-COF

displayed high chemical stability under harsh conditions (9 M HCl (aq.) and 9 M NaOH (aq.)). When Por-sp^2c-COF was applied as a photocatalyst for the visible-light-driven aerobic oxidation of amines, it exhibited extraordinary photocatalytic performance that outperformed many other reported photocatalysts such as g-C_3N_4. Notably, the high chemical stability conferred Por-sp^2c-COF with excellent photocatalytic efficiency under high concentrations of amine, which far outperformed imine-linked por-COF counterpart with respect to reusability and photocatalytic activity. Recently, the same group combined the visible-light absorbing Por-sp^2c-COF with 2,2,6,6-tetramethylpiperidin-1-yl)oxidanyl (TEMPO) as the photocatalyst for the oxidation of amines under the illumination of red LEDs.[111] In contrast to imine-linked Por-COF that was unstable toward benzylamine, Por-sp^2c-COF catalysis achieved high reaction yields from the red-light-induced oxidation of benzylamine in three consecutive runs. These results highlight the potential of robust 2D olefin-linked COF in photocatalysis that involves strong nucleophiles like amines. Along this line, Cai and co-workers constructed an unsubstituted olefin-linked 2D COF (TTO-COF) by an acid-catalyzed Aldol condensation between (4-formylphenyl) triazine and 2,4,6-trimethyl-1,3,5-triazine.[112] Due to the robust olefin linkage, TTO-COF displayed high chemical stability and retained its crystallinity under harsh conditions such as 9 M HCl (aq.) and 9 M NaOH (aq.) for 24 hours. Furthermore, TTO-COF exhibited much better catalytic performance and reusability in photocatalytic degradation of organic dyes and C-H functionalization of arenes and heteroarenes than its imine-linked COF counterpart.

The pronounced chemical stability of COFs also allows the immobilization of catalytic species within COFs for conventional catalytic transformation. As described earlier, in 2018, Cui's group developed a series of chemically robust 2D COFs by manipulating the interlayer steric hindrance.[100] Due to the high chemical robustness and open-pore structure of COFs, the iridium complex could be effectively immobilized onto 2,2′-bipyridyl-based COFs via the post-synthetic metalation. The resulting Ir-COFs catalyzed C-H borylation of arenes efficiently, and the COF decorated with isopropyl groups exhibited much higher activity than that of the COF with ethyl groups and the nonsubstituted COF, which was attributed to the increased porosity and chemical stability. Moreover, the robust Ir-COF catalyst (Ir-4-iPr) was readily recyclable for at least ten consecutive runs and retained high crystallinity and porosity after catalysis. In another example, Yaghi and co-workers immobilized $BF_3{\cdot}OEt_2$ in an olefin-linked COF-701 to heterogenize strong Lewis acid catalyst.[44] The obtained $BF_3{\subset}$COF-701 not only retained crystallinity and porosity but showed high activity in a benchmark Lewis acid-catalyzed Diels-Alder cycloaddition reaction.

3.2 Environmental remediation

Water contamination has been considered as a serious and everlasting threat to the environment and public health. Among several water-treatment methods including coagulation, precipitation, and physical separation, adsorption has emerged as one of the most promising routes on account of its simplicity, low cost, eco-friendliness, and reusability.[113] Compared with porous adsorbents such as activated carbons, zeolites, amorphous organic polymers, and MOFs, COFs are advantageous due to their unique features such as lightweight nature, aligned chelating groups in well-ordered skeletons, continuous nano-channels, and enormous chemical and topological variety.[114]

Mercury (Hg) contamination in aqueous medium has posed a substantial threat to public health. Therefore, the removal of Hg (II) from water to a low concentration is urgently desired. To this end, Jiang's group developed in 2017 a highly stable COF (TAPB-BMTTPA-COF) by integrating methyl sulfide moieties to the pore walls to alleviate the interlayer repulsion.[115] TAPB-BMTTPA-COF was synthesized by the polycondensation of 2,5-bis(methylthio)terephthalaldehyde (BMTTPA) and TAPB with remarkable chemical stability toward hexane, boiling water, 6 M HCl (aq.) and 6 M NaOH (aq.) for 3 days. When implemented as Hg (II) adsorbents, TAPB-BMTTPA COF exhibited unprecedented high performance in removing Hg (II) from aqueous solutions with ultrahigh saturated Hg (II) removal capacity (734 mg g^{-1}) and fast removal rate (5 min), which far surpassed those of previously reported benchmark adsorbents. Moreover, TAPB-BMTTPA COF was readily reused for at least six cycles without significant loss in capacity (92% retention), which outperformed the benchmark adsorbents including MOFs, mesoporous silicas, and porous carbons.

Another notable pollutant is antibiotics that disrupt microbial communities and severely endanger aquatic organisms. To overcome this issue, Fang and co-workers constructed a series of polyarylether-based COFs (PAE-COFs) featuring extremely high chemical stability under harsh conditions.[55] Thanks to the exceptionally high chemical robustness, carboxyl- or amino-functionalized PAE-COFs showed remarkable performance in the removal of antibiotics from water under the pH range of 1-13. Moreover, PAE-COFs were readily reusable for five consecutive cycles in antibiotics removal without obvious loss of capacity. These results suggest that stable PAE-COFs are highly promising adsorbents for antibiotics removal in aqueous mediums with a wide range of pH values.

Besides Hg(II) and antibiotics removal, radionuclides sequestration is also highly demanded in environmental protection.[116] COFs with structural periodicity, customizable porosity, and large surface area hold great promise for extracting radionuclides such as UO_2^{2+}. However, inadequate stability represents a serious bottleneck for aqueous

radionuclides extraction. Recently, Qiu and co-workers developed a highly stable and fluorescent olefin-linked COF, TFPT-BTAN-AO, by Knoevenagel condensation of triazine-based building blocks and subsequent transformation of the nitrile to amidoxime groups (Figure 15).[49] The resulting olefin-linked TFPT-BTAN-AO COF showed excellent chemical stability even in 5 M nitric acid for 12 hours. The abundant selective UO_2^{2+}-chelating groups, amidoxime on the highly accessible and periodic pore walls of COFs empowered COFs with an exceptional UO_2^{2+} adsorption capacity of 427 mg g^{-1}. Given that UO_2^{2+} is mainly present in the acidic environment, the extraction of UO_2^{2+} in harsh conditions is highly desirable for practical applications. TFPT-BTAN-AO showed high adsorption capacity in highly acidic media (3 M HNO_3) with a saturated capacity of 128 mg g^{-1}. Moreover, the uranium extraction performance of TFPT-BTAN-AO remained nearly unaltered after treatment in extreme conditions such as boiling water, 1 M HCl (aq.), 5 M HNO_3 (aq.), 1 M NaOH (aq.), and γ-ray irradiation (200 kGy). TFPT-BTAN-AO could be readily reused six times without comprising uranium extraction performance, making it the first COF capable of regenerable extraction of UO_2^{2+}. These results indicate that robust TFPTBTAN-AO COF holds great potential in practical radionuclides sequestration.

Robust COFs have also spurred tremendous attention in sewage treatment recently. Ma and co-workers prepared a robust superhydrophobic COF (COF-VF) through a post-synthetic attachment of perfluoroalkyl groups onto a COF-V.[106] To circumvent the inadequate processability and avoid handling of COF powders, they immobilized COF onto a melamine foam. Benefiting from the super-hydrophobicity which provides a self-cleaning surface, chemical robustness that retains the frameworks, and hierarchical structures that facilitate substrate diffusion, the obtained compressible COF-VF@foam was used directly as a high-performance sorbent for the removal of organic pollutants with rapid oil-adsorption kinetics. The captured oil was removed by simply squeezing the foam and COF-VF@foam was readily recycled without noticeable loss in its performance, revealing the great potential of COF-VF@foam in practical oil-spill recovery. Following the strategy described above, Zhang and co-workers recently prepared a superhydrophobic COF, COF-DTF, by grafting perfluoroalkyl chains on a hydroxy-functionalized COF via a nucleophilic substitution reaction.[117] The obtained COF-DTF could be deposited onto various substrates including foam, fabric, and glass. These COF-DTF@foam maintained its pristine superhydrophobicity under extreme acidic/basic conditions (pH = 1-14) and boiling water. Notably, it showed high adsorption capacity and recyclability as an adsorbent for oil, even in a continuous separation of the light oil/water mixture, highlighting their great potential in practical sewage treatment.

3.3 Chiral separation

COFs offer a unique platform for accurate molecular sieving due to the customizable crystalline porous architectures. In recent years, significant progress has been made for the exploration of COFs in task-specific separation such as H_2 isotopes separation, CO_2/N_2 separation, homologue separation, and separation of organic molecules.[54] The chiral separation is of prime significance for both fundamental science and industrial applications, such as fine chemicals and pharmaceutical development. In 2018, Cui's group synthesized a chiral 3D COF bearing a 1,3-dioxolane-4,5-dimethanol skeleton, namely CCOF-6, by post-synthetic amidation of imine-linked CCOF-5.[118] The amide-linked CCOF displayed dramatically enhanced chemical stability in 12 M HCl (aq.) and 1 M NaOH (aq.) over 1 day. Amide-linked COF retained its crystallinity while the pristine imine-linked COF was nearly dissolved. Both COFs were tested as chiral stationary phases for high-performance liquid chromatography to enantioselectively separate a series of racemic alcohols (racemic 1-phenyl-2-propanol, 1-phenyl-1-pentanol, 1-phenyl-1-propanol and 1-(4-bromophenyl) ethanol), and the amide-linked COF outperformed the parent imine framework in all cases.

3.4 Corrosive gas sensing

COFs have drawn considerable attention in sensing applications towards various substances such as explosives, metal ions, humidity, gas, and other hazardous species.[62] Among them, the corrosive gas sensing is challenging due to the high demand for the chemical robustness of COFs.

In 2018, Bojdys's group attempted the synthesis of a robust *β*-ketoenamine-linked COF, PBHP-TAPT possessing triazine-moieties.[37] The PBHP-TAPT powder was highly sensitive to a low concentration of HCl gas (20-50 ppm) with a rapid color change from orange to red (Figure 16), which was attributed to the protonation of the triazine nitrogen. Intriguingly, this coloration was fully reversible when the HCl-treated COF was exposed to NH_3 vapor. The sensing capability of COF was readily retained after five consecutive HCl-NH_3 exposure cycles. Due to the irreversible linkage, the PBHP-TAPT COF retained its structural integrity throughout the exposure to HCl and NH_3 vapors. In 2019, Mirica and co-workers synthesized a robust phenazine-fused COF (COF-DC-8).[51] The fully annulated skeletons endowed COF-DC-8 with high bulk conductivity of 2.51×10^{-3} S m^{-1} at room temperature, which was among the highest within reported conductive COFs. COF suspensions were drop-cast onto interdigitated

electrodes to fabricate chemiresistive devices, which showed extraordinary responses to various reducing and oxidizing gases (H_2S, NH_3, NO, and NO_2) with parts-per-billion limits of detection after only 1.5 minutes exposure, significantly outperforming small molecule metal phthalocyanines-based chemiresistors. This study uncovers the high potential of conductive COFs devices in chemical sensing.

3.5 Cathodes in Lithium-Ion Batteries

COFs with the precise integration of redox-active units in periodic and adjustable frameworks have emerged as promising organic cathode materials for lithium-ion batteries.[119] To date, the use of COFs as organic cathodes has been mainly focused on imine-linked COFs. However, the stability issues together with structural limitations of imine COFs severely hinder their practical application in rechargeable batteries. Toward this end, Feng's group developed in 2019 a 2D olefin-linked COF (CCP-HATN) featuring a nitrogen-rich backbone, periodic dual-pore structure, and superb chemical stability.[120] Benefiting from the sp^2-carbon conjugated skeletons, 2D CCP-HATN COF possesses exceptional chemical and electrochemical stabilities. CCP-HATN COF showed high stability in 12 M HCl (aq.) and 12 M NaOH (aq.) without loss of crystallinity, outlasting its imine COF counterpart. Furthermore, after growing 2D CCP-HATN *in situ* on carbon nanotubes (CNTs), the resultant conductive 2D CCP-HATN@CNT composite exhibited a high capacity (116 mAh g^{-1}) and high utilization of redox-active units, with marked cycling stability (91% retention after 1000 cycles) and rate capability (82%, 1.0 A g^{-1} vs. 0.1 A g^{-1}) as an organic cathode for lithium-ion batteries. Most recently, Liu and co-workers developed a robust and crystalline phenazine-fused porous graphitic framework (PGF-1) via a basic hydrothermal synthesis.[54] When employed as cathodes in lithium-ion batteries, PGF-1 displayed record-high specific capacity (842 mAh g^{-1}), excellent cycling durability (stable after 1400 cycles), and electrical conductivity (3.3×10^{-3} S m^{-1}). Notably, the specific capacity of PGF-1 is among the highest for the reported organic cathode materials to date. Moreover, PGF-1 far outperformed the amorphous counterparts concerning capacity and cycle stability, underscoring the importance of high structural regularity for obtaining high electrochemical lithium storage capacity.

Conclusions and Perspectives

In this review, we have summarized recent advances in the development of chemically robust COFs using three main strategies; strengthening covalent linkages using innovative robust linkages, post-synthetic linkage conversion, and post-devitrification; tailoring supramolecular interactions such as intra- and intermolecular H-bonding; mitigating interlayer repulsion as well as manipulating the hydrophobicity and steric hindrance of building blocks. Thanks to the diverse chemistry toolbox that is readily compatible with the reticular synthesis, a growing number of stable COFs have been successfully constructed that can withstand harsh chemical conditions (acidic/alkaline/redox media) relevant to practical applications. With the stability issue being mitigated, the intriguing properties of stable COFs have significantly broadened the scope of COF applications in heterogeneous catalysis, environmental remediation, chiral separation, corrosive gas sensing, and lithium-ion batteries. It is foreseeable that the rapid development of robust COFs will open up new avenues for more diverse applications that require stringent operating conditions.

Despite these remarkable strides, there are considerable challenges and opportunities to be explored:

1) The clear pathway of COFs' structural destruction under various chemical stimuli is still elusive. Therefore, in-depth studies such as *in operando* methods may shed light on the nature of decomposition mechanisms.
2) Each strategy for the synthesis of robust COFs has inherent scope limitations. For instance, *de novo* synthesis of robust COFs via reversible-irreversible cascade reactions requires organic linkers with specific pendant functional groups (e.g., -OH) for further oxidative cyclization; The post-synthetic linkage conversion approach is predominantly applicable for imine-based COFs, thus greatly restricting the scope of the methodology. Developing a facile and more broadly applicable approach is still desirable.
3) The chemical stability of 3D COFs without interlayer π–π stacking is perceived as more problematic than 2D COFs. Research endeavors to develop robust COFs have mainly concentrated on 2D structures, while the exploration of stable 3D COFs remains extremely scarce to date.
4) The chemically robust COFs are mainly obtained as aggregated polycrystalline powders with inadequate processability, which creates severe limitations for both electrocatalytic and optoelectronic applications. Fabrication of robust COFs films is highly appealing yet the relevant study is still in its nascent stage and worth further efforts. Post-synthetic modifications may provide a unique opportunity to concurrently enhance both the stability and the solution processability of COFs.
5) The mechanical stability and scaleup synthesis of robust COFs are both of paramount importance for their potential industrial and commercial implementations. Minimal studies have been conducted to date. The

development of new and robust linkage chemistry may open up more economical paths to scaled materials synthesis from the use of cheaper starting materials.

Such opportunities and challenges will continue to place the designed synthesis of novel chemically stable COFs at the forefront of materials research. The stability limit of COFs shall be further pushed to compete with potential contenders such as zeolites and mesoporous silica. It is worth noting that the lack of unified standards to assess chemical stability (e.g., exposure time, quantity, temperature, and characterizations) makes it problematic to quantitatively evaluate stability across different systems. Therefore, it would be helpful to establish a standard benchmark by which to assess the chemical stabilities of COFs. Looking forward, the exploration of new robust yet dynamic chemical bonds which are typically considered as static under normal conditions (such as C=N bonds in triazine and pyrazine), and post-synthetic linkage conversion of pre-established COFs beyond imine linkages will bear more fruitful breakthroughs in the discovery of COFs with exceptional chemical robustness. Additionally, the predictive power of computational chemistry is expected to guide an accelerated discovery of functional, stable COFs when combined with robotic synthesis. Researchers will benefit from an automated or even autonomous workflow, instead of the laborious trial-and-error approach, to navigate through a maximum set of structural complexity, reactivity, and synthetic conditions for the synthesis of robust COFs. Moreover, in-depth mechanistic elucidations of specialized applications are also highly desirable for stable COFs. Future developments in these aspects will grant numerous possibilities for multidisciplinary applications of these functionally boosted COFs.

ACKNOWLEDGMENTS

We gratefully acknowledge the financial support from the Molecular Foundry, Lawrence Berkeley National Laboratory, a user facility supported by the Office of Science, Office of Basic Energy Sciences, of the U.S. Department of Energy under contract no. DE-AC02-05CH11231. X.L. and Y.L. acknowledge the support from the U.S. Department of Energy, Office of Science, Office of Basic Energy Sciences, Materials Sciences and Engineering Division, under Contract No. DE-AC02-05-CH11231 within the Inorganic/Organic Nanocomposites Program (KC3104).

AUTHOR CONTRIBUTIONS

Conceptualization, X.L., and Y.L.; Investigation, X.L., and S.C.; Writing-Original Draft, X.L., S.C., B.S., and C.Y.; Review & Revision, J. Z., and Y.L.; Funding Acquisition, Y.L.; Supervision, Y.L.

REFERENCES

1. Cote, A.P., Benin, A.I., Ockwig, N.W., O'Keeffe, M., Matzger, A.J., and Yaghi, O.M. (2005). Porous, crystalline, covalent organic frameworks. Science *310*, 1166-1170.
2. Diercks, C.S., and Yaghi, O.M. (2017). The atom, the molecule, and the covalent organic framework. Science *355*, eaal1585.
3. Bisbey, R.P., and Dichtel, W.R. (2017). Covalent organic frameworks as a platform for multidimensional polymerization. ACS Cent. Sci. *3*, 533-543.
4. Huang, N., Wang, P., and Jiang, D. (2016). Covalent organic frameworks: a materials platform for structural and functional designs. Nat. Rev. Mater. *1*, 16068.
5. Chen, X., Geng, K., Liu, R., Tan, K.T., Gong, Y., Li, Z., Tao, S., Jiang, Q., and Jiang, D. (2020). Covalent Organic Frameworks: Chemical Approaches to Designer Structures and Built-In Functions. Angew. Chem. Int. Ed. *59*, 5050-5091.
6. Ghazi, Z.A., Zhu, L., Wang, H., Naeem, A., Khattak, A.M., Liang, B., Khan, N.A., Wei, Z., Li, L., and Tang, Z. (2016). Efficient Polysulfide Chemisorption in Covalent Organic Frameworks for High-Performance Lithium-Sulfur Batteries. Adv. Energy Mater. *6*, 1601250.
7. Shi, Y., Zhang, X., Liu, H., Han, J., Yang, Z., Gu, L., and Tang, Z. (2020). Metalation of Catechol-Functionalized Defective Covalent Organic Frameworks for Lewis Acid Catalysis. Small *16*, 2001998.
8. Smith, B.J., Overholts, A.C., Hwang, N., and Dichtel, W.R. (2016). Insight into the crystallization of amorphous imine-linked polymer networks to 2D covalent organic frameworks. Chem.Comm. *52*, 3690-3693.
9. Vitaku, E., and Dichtel, W.R. (2017). Synthesis of 2D Imine-Linked Covalent Organic Frameworks through Formal Transimination Reactions. J. Am. Chem. Soc. *139*, 12911-12914.
10. Zhai, Y., Liu, G., Jin, F., Zhang, Y., Gong, X., Miao, Z., Li, J., Zhang, M., Cui, Y., and Zhang, L. (2019). Construction of Covalent ‐ Organic Frameworks (COFs) from Amorphous Covalent Organic Polymers via Linkage Replacement. Angew. Chem. Int. Ed. *58*, 17679-17683.

11. Li, X., Yang, C., Sun, B., Cai, S., Chen, Z., Lv, Y., Zhang, J., and Liu, Y. (2020). Expeditious Synthesis of Covalent Organic Frameworks: A Review. J. Mater. Chem. A. *8*, 16045-16060.
12. Song, Y., Sun, Q., Aguila, B., and Ma, S. (2019). Opportunities of covalent organic frameworks for advanced applications. Adv. Sci. *6*, 1801410.
13. Ding, S.-Y., and Wang, W. (2013). Covalent organic frameworks (COFs): from design to applications. Chem. Soc. Rev. *42*, 548-568.
14. Lohse, M.S., and Bein, T. (2018). Covalent organic frameworks: structures, synthesis, and applications. Adv. Funct. Mater. *28*, 1705553.
15. Alahakoon, S.B., Diwakara, S.D., Thompson, C.M., and Smaldone, R.A. (2020). Supramolecular design in 2D covalent organic frameworks. Chem. Soc. Rev. *49*, 1344-1356.
16. Lyle, S.J., Waller, P.J., and Yaghi, O.M. (2019). Covalent Organic Frameworks: Organic Chemistry Extended into Two and Three Dimensions. Trends Chem. *1*, 172-184.
17. Wang, H., Zeng, Z., Xu, P., Li, L., Zeng, G., Xiao, R., Tang, Z., Huang, D., Tang, L., Lai, C.*, et al.* (2019). Recent progress in covalent organic framework thin films: fabrications, applications and perspectives. Chem. Soc. Rev. *48*, 488-516.
18. Wang, Z., Zhang, S., Chen, Y., Zhang, Z., and Ma, S. (2020). Covalent organic frameworks for separation applications. Chem. Soc. Rev. *49*, 708-735.
19. Liu, X., Huang, D., Lai, C., Zeng, G., Qin, L., Wang, H., Yi, H., Li, B., Liu, S., Zhang, M.*, et al.* (2019). Recent advances in covalent organic frameworks (COFs) as a smart sensing material. Chem. Soc. Rev. *48*, 5266-5302.
20. Sharma, R.K., Yadav, P., Yadav, M., Gupta, R., Rana, P., Srivastava, A., Zbořil, R., Varma, R.S., Antonietti, M., and Gawande, M.B. (2020). Recent development of covalent organic frameworks (COFs): synthesis and catalytic (organic-electro-photo) applications. Mater. Horiz. *7*, 411-454.
21. Beaudoin, D., Maris, T., and Wuest, J.D. (2013). Constructing monocrystalline covalent organic networks by polymerization. Nat. Chem. *5*, 830-834.
22. Geng, K., He, T., Liu, R., Tan, K.T., Li, Z., Tao, S., Gong, Y., Jiang, Q., and Jiang, D. (2020). Covalent Organic Frameworks: Design, Synthesis, and Functions. Chem. Rev. *120*, 8814-8933.
23. Ding, S.-Y., Gao, J., Wang, Q., Zhang, Y., Song, W.-G., Su, C.-Y., and Wang, W. (2011). Construction of covalent organic framework for catalysis: Pd/COF-LZU1 in Suzuki–Miyaura coupling reaction. J. Am. Chem. Soc. *133*, 19816-19822.
24. Dalapati, S., Jin, S., Gao, J., Xu, Y., Nagai, A., and Jiang, D. (2013). An Azine-Linked Covalent Organic Framework. J. Am. Chem. Soc. *135*, 17310-17313.
25. Kuhn, P., Antonietti, M., and Thomas, A. (2008). Porous, Covalent Triazine-Based Frameworks Prepared by Ionothermal Synthesis. Angew. Chem. Int. Ed. *47*, 3450-3453.
26. Li, Y., Wang, C., Ma, S., Zhang, H., Ou, J., Wei, Y., and Ye, M. (2019). Fabrication of Hydrazone-Linked Covalent Organic Frameworks Using Alkyl Amine as Building Block for High Adsorption Capacity of Metal Ions. ACS Appl. Mater. Interfaces *11*, 11706-11714.
27. Zhang, K., Cai, S.-L., Yan, Y.-L., He, Z.-H., Lin, H.-M., Huang, X.-L., Zheng, S.-R., Fan, J., and Zhang, W.-G. (2017). Construction of a hydrazone-linked chiral covalent organic framework–silica composite as the stationary phase for high performance liquid chromatography. J. Chromatogr. A *1519*, 100-109.
28. Nagai, A., Chen, X., Feng, X., Ding, X., Guo, Z., and Jiang, D. (2013). A Squaraine-Linked Mesoporous Covalent Organic Framework. Angew. Chem. Int. Ed. *52*, 3770-3774.
29. Fang, Q., Zhuang, Z., Gu, S., Kaspar, R.B., Zheng, J., Wang, J., Qiu, S., and Yan, Y. (2014). Designed synthesis of large-pore crystalline polyimide covalent organic frameworks. Nat. Commun. *5*, 4503.
30. Kandambeth, S., Mallick, A., Lukose, B., Mane, M.V., Heine, T., and Banerjee, R. (2012). Construction of crystalline 2D covalent organic frameworks with remarkable chemical (acid/base) stability via a combined reversible and irreversible route. J. Am. Chem. Soc. *134*, 19524-19527.
31. Zhuang, X., Zhao, W., Zhang, F., Cao, Y., Liu, F., Bi, S., and Feng, X. (2016). A two-dimensional conjugated polymer framework with fully sp 2-bonded carbon skeleton. Polym. Chem. *7*, 4176-4181.
32. Zhao, C., Diercks, C.S., Zhu, C., Hanikel, N., Pei, X., and Yaghi, O.M. (2018). Urea-linked covalent organic frameworks. J. Am. Chem. Soc. *140*, 16438-16441.
33. Zhang, B., Wei, M., Mao, H., Pei, X., Alshmimri, S.A., Reimer, J.A., and Yaghi, O.M. (2018). Crystalline dioxin-linked covalent organic frameworks from irreversible reactions. J. Am. Chem. Soc. *140*, 12715-12719.
34. Uribe-Romo, F.J., Hunt, J.R., Furukawa, H., Klock, C., O'Keeffe, M., and Yaghi, O.M. (2009). A crystalline imine-linked 3-D porous covalent organic framework. J. Am. Chem. Soc. *131*, 4570-4571.
35. Segura, J.L., Mancheño, M.J., and Zamora, F. (2016). Covalent organic frameworks based on Schiff-base chemistry: synthesis, properties and potential applications. Chem. Soc. Rev. *45*, 5635-5671.

36. Rao, M.R., Fang, Y., De Feyter, S., and Perepichka, D.F. (2017). Conjugated covalent organic frameworks via michael addition–elimination. J. Am. Chem. Soc. *139*, 2421-2427.
37. Kulkarni, R., Noda, Y., Barange, D.K., Kochergin, Y.S., Lyu, P., Balcarova, B., Nachtigall, P., and Bojdys, M. (2019). Real-time optical and electronic sensing with a β-amino enone linked, triazine-containing 2D covalent organic framework. Nat. Commun. *10*, 3228.
38. Liu, Y., Wang, Y., Li, H., Guan, X., Zhu, L., Xue, M., Yan, Y., Valtchev, V., Qiu, S., and Fang, Q. (2019). Ambient aqueous-phase synthesis of covalent organic frameworks for degradation of organic pollutants. Chem. Sci. *10*, 10815-10820.
39. Acharjya, A., Pachfule, P., Roeser, J., Schmitt, F.J., and Thomas, A. (2019). Vinylene-Linked Covalent Organic Frameworks by Base-Catalyzed Aldol Condensation. Angew. Chem. Int. Ed. *58*, 14865-14870.
40. Jin, E., Asada, M., Xu, Q., Dalapati, S., Addicoat, M.A., Brady, M.A., Xu, H., Nakamura, T., Heine, T., and Chen, Q. (2017). Two-dimensional sp2 carbon–conjugated covalent organic frameworks. Science *357*, 673-676.
41. Jin, E., Lan, Z., Jiang, Q., Geng, K., Li, G., Wang, X., and Jiang, D. (2019). 2D sp2 carbon-conjugated covalent organic frameworks for photocatalytic hydrogen production from water. Chem *5*, 1632-1647.
42. Jin, E., Li, J., Geng, K., Jiang, Q., Xu, H., Xu, Q., and Jiang, D. (2018). Designed synthesis of stable light-emitting two-dimensional sp 2 carbon-conjugated covalent organic frameworks. Nat. Commun. *9*, 4143.
43. Jadhav, T., Fang, Y., Patterson, W., Liu, C.H., Hamzehpoor, E., and Perepichka, D.F. (2019). 2D poly (arylene vinylene) covalent organic frameworks via aldol condensation of trimethyltriazine. Angew. Chem. Int. Ed. *58*, 13753-13757.
44. Lyu, H., Diercks, C.S., Zhu, C., and Yaghi, O.M. (2019). Porous crystalline olefin-linked covalent organic frameworks. J. Am. Chem. Soc. *141*, 6848-6852.
45. Wei, S., Zhang, F., Zhang, W., Qiang, P., Yu, K., Fu, X., Wu, D., Bi, S., and Zhang, F. (2019). Semiconducting 2D Triazine-cored covalent organic frameworks with unsubstituted olefin linkages. J. Am. Chem. Soc. *141*, 14272-14279.
46. Bi, S., Yang, C., Zhang, W., Xu, J., Liu, L., Wu, D., Wang, X., Han, Y., Liang, Q., and Zhang, F. (2019). Two-dimensional semiconducting covalent organic frameworks via condensation at arylmethyl carbon atoms. Nat. Commun. *10*, 2467.
47. Fu, Z., Wang, X., Gardner, A.M., Wang, X., Chong, S.Y., Neri, G., Cowan, A.J., Liu, L., Li, X., Vogel, A.*, et al.* (2020). A stable covalent organic framework for photocatalytic carbon dioxide reduction. Chem. Sci. *11*, 543-550.
48. Xu, J., He, Y., Bi, S., Wang, M., Yang, P., Wu, D., Wang, J., and Zhang, F. (2019). An Olefin-Linked Covalent Organic Framework as a Flexible Thin-Film Electrode for a High-Performance Micro-Supercapacitor. Angew. Chem. Int. Ed. *131*, 12193-12197.
49. Cui, W.-R., Zhang, C.-R., Jiang, W., Li, F.-F., Liang, R.-P., Liu, J., and Qiu, J.-D. (2020). Regenerable and stable sp 2 carbon-conjugated covalent organic frameworks for selective detection and extraction of uranium. Nat. Commun. *11*, 436.
50. Huang, N., Lee, K.H., Yue, Y., Xu, X., Irle, S., Jiang, Q., and Jiang, D. (2020). A Stable and Conductive Metallophthalocyanine Framework for Electrocatalytic Carbon Dioxide Reduction in Water. Angew. Chem. Int. Ed. *59*, 2-9.
51. Meng, Z., Stolz, R.M., and Mirica, K.A. (2019). Two-Dimensional Chemiresistive Covalent Organic Framework with High Intrinsic Conductivity. J. Am. Chem. Soc. *141*, 11929-11937.
52. Kou, Y., Xu, Y., Guo, Z., and Jiang, D. (2011). Supercapacitive Energy Storage and Electric Power Supply Using an Aza-Fused π-Conjugated Microporous Framework. Angew. Chem. Int. Ed. *50*, 8753-8757.
53. Marco, A.B., Cortizo-Lacalle, D., Perez-Miqueo, I., Valenti, G., Boni, A., Plas, J., Strutyński, K., De Feyter, S., Paolucci, F., and Montes, M. (2017). Twisted Aromatic Frameworks: Readily Exfoliable and Solution-Processable Two-Dimensional Conjugated Microporous Polymers. Angew. Chem. Int. Ed. *56*, 6946-6951.
54. Li, X., Wang, H., Chen, H., Zheng, Q., Zhang, Q., Mao, H., Liu, Y., Cai, S., Sun, B., and Dun, C. (2020). Dynamic covalent synthesis of crystalline porous graphitic frameworks. Chem *6*, 933-944.
55. Guan, X., Li, H., Ma, Y., Xue, M., Fang, Q., Yan, Y., Valtchev, V., and Qiu, S. (2019). Chemically stable polyarylether-based covalent organic frameworks. Nat. Chem. *11*, 587-594.
56. Ben-Haida, A., Baxter, I., M. Colquhoun, H., Hodge, P., H. Kohnke, F., and J. Williams, D. (1997). Ring-closing depolymerisation of aromatic polyethers. Chem.Comm., 1533-1534.
57. Ong, W.J., and Swager, T.M. (2018). Dynamic self-correcting nucleophilic aromatic substitution. Nat. Chem. *10*, 1023-1030.

58. Biswal, B.P., Vignolo-González, H.A., Banerjee, T., Grunenberg, L., Savasci, G., Gottschling, K., Nuss, J., Ochsenfeld, C., and Lotsch, B.V. (2019). Sustained Solar H2 Evolution from a Thiazolo[5,4-d]thiazole-Bridged Covalent Organic Framework and Nickel-Thiolate Cluster in Water. J. Am. Chem. Soc. *141*, 11082-11092.
59. Sun, Q., Aguila, B., Earl, L.D., Abney, C.W., Wojtas, L., Thallapally, P.K., and Ma, S. (2018). Covalent organic frameworks as a decorating platform for utilization and affinity enhancement of chelating sites for radionuclide sequestration. Adv. Mater. *30*, 1705479.
60. Mulzer, C.R., Shen, L., Bisbey, R.P., McKone, J.R., Zhang, N., Abruña, H.D., and Dichtel, W.R. (2016). Superior Charge Storage and Power Density of a Conducting Polymer-Modified Covalent Organic Framework. ACS Cent. Sci. *2*, 667-673.
61. Ma, H., Liu, B., Li, B., Zhang, L., Li, Y.-G., Tan, H.-Q., Zang, H.-Y., and Zhu, G. (2016). Cationic Covalent Organic Frameworks: A Simple Platform of Anionic Exchange for Porosity Tuning and Proton Conduction. J. Am. Chem. Soc. *138*, 5897-5903.
62. Liu, M., Guo, L., Jin, S., and Tan, B. (2019). Covalent triazine frameworks: synthesis and applications. J. Mater. Chem. A *7*, 5153-5172.
63. Liu, M., Jiang, K., Ding, X., Wang, S., Zhang, C., Liu, J., Zhan, Z., Cheng, G., Li, B., and Chen, H. (2019). Controlling monomer feeding rate to achieve highly crystalline covalent triazine frameworks. Adv. Mater. *31*, 1807865.
64. Wang, K., Yang, L.M., Wang, X., Guo, L., Cheng, G., Zhang, C., Jin, S., Tan, B., and Cooper, A. (2017). Covalent Triazine Frameworks via a Low-Temperature Polycondensation Approach. Angew. Chem. Int. Ed. *56*, 14149-14153.
65. Liu, M., Huang, Q., Wang, S., Li, Z., Li, B., Jin, S., and Tan, B. (2018). Crystalline covalent triazine frameworks by in situ oxidation of alcohols to aldehyde monomers. Angew. Chem. Int. Ed. *57*, 11968-11972.
66. Zhang, S., Cheng, G., Guo, L., Wang, N., Tan, B., and Jin, S. (2020). Strong-Base-Assisted Synthesis of a Crystalline Covalent Triazine Framework with High Hydrophilicity via Benzylamine Monomer for Photocatalytic Water Splitting. Angew. Chem. Int. Ed. *59*, 6007-6014.
67. Wei, P.-F., Qi, M.-Z., Wang, Z.-P., Ding, S.-Y., Yu, W., Liu, Q., Wang, L.-K., Wang, H.-Z., An, W.-K., and Wang, W. (2018). Benzoxazole-linked ultrastable covalent organic frameworks for photocatalysis. J. Am. Chem. Soc. *140*, 4623-4631.
68. Pyles, D.A., Crowe, J.W., Baldwin, L.A., and McGrier, P.L. (2016). Synthesis of Benzobisoxazole-Linked Two-Dimensional Covalent Organic Frameworks and Their Carbon Dioxide Capture Properties. ACS Macro Lett. *5*, 1055-1058.
69. Wang, P.-L., Ding, S.-Y., Zhang, Z.-C., Wang, Z.-P., and Wang, W. (2019). Constructing Robust Covalent Organic Frameworks via Multicomponent Reactions. J. Am. Chem. Soc. *141*, 18004-18008.
70. Ranjeesh, K.C., Illathvalappil, R., Veer, S.D., Peter, J., Wakchaure, V.C., Goudappagouda, Raj, K.V., Kurungot, S., and Babu, S.S. (2019). Imidazole-Linked Crystalline Two-Dimensional Polymer with Ultrahigh Proton-Conductivity. J. Am. Chem. Soc. *141*, 14950-14954.
71. Li, T., Yan, X., Liu, Y., Zhang, W.-D., Fu, Q.-T., Zhu, H., Li, Z., and Gu, Z.-G. (2020). A 2D covalent organic framework involving strong intramolecular hydrogen bonds for advanced supercapacitors. Polym. Chem. *11*, 47-52.
72. Wang, K., Jia, Z., Bai, Y., Wang, X., Hodgkiss, S.E., Chen, L., Chong, S.Y., Wang, X., Yang, H., Xu, Y.*, et al.* (2020). Synthesis of Stable Thiazole-Linked Covalent Organic Frameworks via a Multicomponent Reaction. J. Am. Chem. Soc. *142*, 11131-11138.
73. Li, X.-T., Zou, J., Wang, T.-H., Ma, H.-C., Chen, G.-J., and Dong, Y.-B. (2020). Construction of Covalent Organic Frameworks via Three-Component One-Pot Strecker and Povarov Reactions. J. Am. Chem. Soc. *142*, 6521-6526.
74. Li, C., Ma, Y., Liu, H., Tao, L., Ren, Y., Chen, X., Li, H., and Yang, Q. (2020). Asymmetric photocatalysis over robust covalent organic frameworks with tetrahydroquinoline linkage. Chinese J. Catal. *41*, 1288-1297.
75. Su, Y., Wan, Y., Xu, H., Otake, K.-i., Tang, X., Huang, L., Kitagawa, S., and Gu, C. (2020). Crystalline and Stable Benzofuran-Linked Covalent Organic Frameworks from Irreversible Cascade Reactions. J. Am. Chem. Soc. *142*, 13316-13321.
76. Segura, J.L., Royuela, S., and Ramos, M.M. (2019). Post-synthetic modification of covalent organic frameworks. Chem. Soc. Rev. *48*, 3903-3945.
77. Ding, H., Mal, A., and Wang, C. (2020). Tailored covalent organic frameworks by post-synthetic modification. Mater. Chem. Front. *4*, 113-127.

78. Jadhav, T., Fang, Y., Liu, C.-H., Dadvand, A., Hamzehpoor, E., Patterson, W., Jonderian, A., Stein, R.S., and Perepichka, D.F. (2020). Transformation between 2D and 3D Covalent Organic Frameworks via Reversible [2 + 2] Cycloaddition. J. Am. Chem. Soc. *142*, 8862-8870.
79. Waller, P.J., Lyle, S.J., Osborn Popp, T.M., Diercks, C.S., Reimer, J.A., and Yaghi, O.M. (2016). Chemical conversion of linkages in covalent organic frameworks. J. Am. Chem. Soc. *138*, 15519-15522.
80. Haase, F., Troschke, E., Savasci, G., Banerjee, T., Duppel, V., Dörfler, S., Grundei, M.M., Burow, A.M., Ochsenfeld, C., and Kaskel, S. (2018). Topochemical conversion of an imine-into a thiazole-linked covalent organic framework enabling real structure analysis. Nat. Commun. *9*, 2600.
81. Waller, P.J., AlFaraj, Y.S., Diercks, C.S., Jarenwattananon, N.N., and Yaghi, O.M. (2018). Conversion of imine to oxazole and thiazole linkages in covalent organic frameworks. J. Am. Chem. Soc. *140*, 9099-9103.
82. Lyle, S.J., Osborn Popp, T.M., Waller, P.J., Pei, X., Reimer, J.A., and Yaghi, O.M. (2019). Multistep Solid-State Organic Synthesis of Carbamate-Linked Covalent Organic Frameworks. J. Am. Chem. Soc. *141*, 11253-11258.
83. Seo, J.-M., Noh, H.-J., Jeong, H.Y., and Baek, J.-B. (2019). Converting Unstable Imine-Linked Network into Stable Aromatic Benzoxazole-Linked One via Post-oxidative Cyclization. J. Am. Chem. Soc. *141*, 11786-11790.
84. Wang, Y., Liu, H., Pan, Q., Wu, C., Hao, W., Xu, J., Chen, R., Liu, J., Li, Z., and Zhao, Y. (2020). Construction of Fully Conjugated Covalent Organic Frameworks via Facile Linkage Conversion for Efficient Photoenzymatic Catalysis. J. Am. Chem. Soc. *142*, 5958-5963.
85. Liu, H., Chu, J., Yin, Z., Cai, X., Zhuang, L., and Deng, H. (2018). Covalent organic frameworks linked by amine bonding for concerted electrochemical reduction of CO2. Chem *4*, 1696-1709.
86. Li, X., Zhang, C., Cai, S., Lei, X., Altoe, V., Hong, F., Urban, J.J., Ciston, J., Chan, E.M., and Liu, Y. (2018). Facile transformation of imine covalent organic frameworks into ultrastable crystalline porous aromatic frameworks. Nat. Commun. *9*, 2998.
87. Qian, H.-L., Meng, F.-L., Yang, C.-X., and Yan, X.-P. (2020). Irreversible amide-linked covalent organic framework for selective and ultrafast gold recovery. Angew. Chem. Int. Ed. Online date: July 04, 2020. DOI: doi.org/10.1002/anie.202006535
88. Stewart, D., Antypov, D., Dyer, M.S., Pitcher, M.J., Katsoulidis, A.P., Chater, P.A., Blanc, F., and Rosseinsky, M. (2017). Stable and ordered amide frameworks synthesised under reversible conditions which facilitate error checking. Nat. Commun. *8*, 1102.
89. Unterlass, M.M. (2018). Hot Water Generates Crystalline Organic Materials. Angew. Chem. Int. Ed. *57*, 2292-2294.
90. Li, H., Li, H., Dai, Q., Li, H., and Brédas, J.-L. (2018). Hydrolytic Stability of Boronate Ester-Linked Covalent Organic Frameworks. Adv. Theory Simul. *1*, 1700015.
91. Du, Y., Mao, K., Kamakoti, P., Ravikovitch, P., Paur, C., Cundy, S., Li, Q., and Calabro, D. (2012). Experimental and computational studies of pyridine-assisted post-synthesis modified air stable covalent–organic frameworks. Chem.Comm. *48*, 4606-4608.
92. Du, Y., Calabro, D., Wooler, B., Kortunov, P., Li, Q., Cundy, S., and Mao, K. (2015). One step facile synthesis of amine-functionalized COF-1 with enhanced hydrostability. Chem. Mater. *27*, 1445-1447.
93. Zhang, G., Li, X., Liao, Q., Liu, Y., Xi, K., Huang, W., and Jia, X. (2018). Water-dispersible PEG-curcumin/amine-functionalized covalent organic framework nanocomposites as smart carriers for in vivo drug delivery. Nat. Commun. *9*, 2785.
94. Chen, X., Addicoat, M., Jin, E., Zhai, L., Xu, H., Huang, N., Guo, Z., Liu, L., Irle, S., and Jiang, D. (2015). Locking Covalent Organic Frameworks with Hydrogen Bonds: General and Remarkable Effects on Crystalline Structure, Physical Properties, and Photochemical Activity. J. Am. Chem. Soc. *137*, 3241-3247.
95. Kandambeth, S., Shinde, D.B., Panda, M.K., Lukose, B., Heine, T., and Banerjee, R. (2013). Enhancement of chemical stability and crystallinity in porphyrin-containing covalent organic frameworks by intramolecular hydrogen bonds. Angew. Chem. Int. Ed. *52*, 13052-13056.
96. Kandambeth, S., Venkatesh, V., Shinde, D.B., Kumari, S., Halder, A., Verma, S., and Banerjee, R. (2015). Self-templated chemically stable hollow spherical covalent organic framework. Nat. Commun. *6*, 6786.
97. Halder, A., Karak, S., Addicoat, M., Bera, S., Chakraborty, A., Kunjattu, S.H., Pachfule, P., Heine, T., and Banerjee, R. (2018). Ultrastable imine-based covalent organic frameworks for sulfuric acid recovery: an effect of interlayer hydrogen bonding. Angew. Chem. Int. Ed. *57*, 5797-5802.
98. Xu, H., Gao, J., and Jiang, D. (2015). Stable, crystalline, porous, covalent organic frameworks as a platform for chiral organocatalysts. Nat. Chem. *7*, 905.
99. Tao, S., Zhai, L., Dinga Wonanke, A.D., Addicoat, M.A., Jiang, Q., and Jiang, D. (2020). Confining H3PO4 network in covalent organic frameworks enables proton super flow. Nat. Commun. *11*, 1981.

100. Wu, X., Han, X., Liu, Y., Liu, Y., and Cui, Y. (2018). Control interlayer stacking and chemical stability of two-dimensional covalent organic frameworks via steric tuning. J. Am. Chem. Soc. *140*, 16124-16133.
101. Zhang, W., Hu, Y., Ge, J., Jiang, H.-L., and Yu, S.-H. (2014). A Facile and General Coating Approach to Moisture/Water-Resistant Metal–Organic Frameworks with Intact Porosity. J. Am. Chem. Soc. *136*, 16978-16981.
102. Li, Y., Chen, Q., Xu, T., Xie, Z., Liu, J., Yu, X., Ma, S., Qin, T., and Chen, L. (2019). De Novo Design and Facile Synthesis of 2D Covalent Organic Frameworks: A Two-in-One Strategy. J. Am. Chem. Soc. *141*, 13822-13828.
103. Yan, X., Liu, H., Li, Y., Chen, W., Zhang, T., Zhao, Z., Xing, G., and Chen, L. (2019). Ultrastable Covalent Organic Frameworks via Self-Polycondensation of an A2B2 Monomer for Heterogeneous Photocatalysis. Macromolecules *52*, 7977-7983.
104. Wu, X., Hong, Y.-l., Xu, B., Nishiyama, Y., Jiang, W., Zhu, J., Zhang, G., Kitagawa, S., and Horike, S. (2020). Perfluoroalkyl-functionalized Covalent Organic Frameworks with Superhydrophobicity for Anhydrous Proton Conduction. J. Am. Chem. Soc. *142*, 14357–14364.
105. Ma, Y., Wang, Y., Li, H., Guan, X., Li, B., Xue, M., Yan, Y., Valtchev, V., Qiu, S., and Fang, Q. (2020). Three-Dimensional Chemically Stable Covalent Organic Frameworks through Hydrophobic Engineering. Angew. Chem. Int. Ed. *59*, 1-7.
106. Sun, Q., Aguila, B., Perman, J.A., Butts, T., Xiao, F.-S., and Ma, S. (2018). Integrating superwettability within covalent organic frameworks for functional coating. Chem *4*, 1726-1739.
107. Liu, J., Wang, N., and Ma, L. (2020). Recent Advances in Covalent Organic Frameworks for Catalysis. Chem. Asian J. *15*, 338-351.
108. Wang, G.-B., Li, S., Yan, C.-X., Zhu, F.-C., Lin, Q.-Q., Xie, K.-H., Geng, Y., and Dong, Y.-B. (2020). Covalent organic frameworks: emerging high-performance platforms for efficient photocatalytic applications. J. Mater. Chem. A *8*, 6957-6983.
109. Bi, S., Thiruvengadam, P., Wei, S., Zhang, W., Zhang, F., Gao, L., Xu, J., Wu, D., Chen, J.-S., and Zhang, F. (2020). Vinylene-Bridged Two-Dimensional Covalent Organic Frameworks via Knoevenagel Condensation of Tricyanomesitylene. J. Am. Chem. Soc. *142*, 11893-11900.
110. Chen, R., Shi, J.-L., Ma, Y., Lin, G., Lang, X., and Wang, C. (2019). Designed Synthesis of a 2D Porphyrin-Based sp2 Carbon-Conjugated Covalent Organic Framework for Heterogeneous Photocatalysis. Angew. Chem. Int. Ed. *58*, 6430-6434.
111. Shi, J.-L., Chen, R., Hao, H., Wang, C., and Lang, X. (2020). 2D sp2 Carbon-Conjugated Porphyrin Covalent Organic Framework for Cooperative Photocatalysis with TEMPO. Angew. Chem. Int. Ed. *59*, 9088-9093.
112. Yang, Y., Niu, H., Xu, L., Zhang, H., and Cai, Y. (2020). Triazine functionalized fully conjugated covalent organic framework for efficient photocatalysis. Appl. Catal., B *269*, 118799.
113. Samanta, P., Desai, A.V., Let, S., and Ghosh, S.K. (2019). Advanced porous materials for sensing, capture and detoxification of organic pollutants toward water remediation. ACS Sustainable Chem. Eng. *7*, 7456-7478.
114. Fernandes, S.P., Romero, V., Espiña, B., and Salonen, L.M. (2019). Tailoring Covalent Organic Frameworks To Capture Water Contaminants. Chem. Eur. J. *25*, 6461-6473.
115. Huang, N., Zhai, L., Xu, H., and Jiang, D. (2017). Stable Covalent Organic Frameworks for Exceptional Mercury Removal from Aqueous Solutions. J. Am. Chem. Soc. *139*, 2428-2434.
116. Sun, Q., Aguila, B., and Ma, S. (2019). Opportunities of porous organic polymers for radionuclide sequestration. Trends Chem. *1*, 292-303.
117. Han, N., Zhang, Z., Gao, H., Qian, Y., Tan, L., Yang, C., Zhang, H., Cui, Z., Li, W., and Zhang, X. (2020). Superhydrophobic Covalent Organic Frameworks Prepared via Pore Surface Modifications for Functional Coatings under Harsh Conditions. ACS Appl. Mater. Interfaces *12*, 2926-2934.
118. Han, X., Huang, J., Yuan, C., Liu, Y., and Cui, Y. (2018). Chiral 3D covalent organic frameworks for high performance liquid chromatographic enantioseparation. J. Am. Chem. Soc. *140*, 892-895.
119. Sun, T., Xie, J., Guo, W., Li, D.-S., and Zhang, Q. (2020). Covalent–Organic Frameworks: Advanced Organic Electrode Materials for Rechargeable Batteries. Adv. Energy Mater. *10*, 1904199.
120. Xu, S., Wang, G., Biswal, B.P., Addicoat, M., Paasch, S., Sheng, W., Zhuang, X., Brunner, E., Heine, T., and Berger, R., and Feng, X. (2019). A Nitrogen-Rich 2D sp2-Carbon-Linked Conjugated Polymer Framework as a High-Performance Cathode for Lithium-Ion Batteries. Angew. Chem. Int. Ed. *131*, 859-863.

Scheme Titles

Scheme 1. The development of chemically robust COFs via various strategies and their widespread applications.
Scheme 2. Representative synthetic progress of chemically robust COFs outlined in chronicle order since 2005.

Figure Titles

Figure 1. Linkages explored for the synthesis of COFs since 2005.
Figure 2. (A) Syntheses of sp^2c-COF through condensation of TFPPy and PDAN, sp^2c-COF-2 through condensation of TFPPy and BPDAN and sp^2c-COF-3 through condensation of TFPPy and TPDAN. (B), (D), (F) are reconstructed single layer crystal structures, and (C), (E), (G) are the corresponding many layer structures of *sp*2c-COF, sp^2c-COF-2, and sp^2c-COF-3, respectively. Reprinted with permission from Jin et al.[42] Copyright 2018, Springer Nature.
Figure 3. (A) Synthesis of crystalline PGF-1 via basic aqueous conditions. (B) The HRTEM image of PGF-1 showing the highly ordered layer of PGF-1. Reprinted with permission from Li et al.[54] Copyright 2020, Elsevier Inc.
Figure 4. Schematics for the synthesis of dioxin-linked COFs COF-318, COF-316 (JUC-505), and JUC-506 through S_NAr reactions.
Figure 5. Schematics for the synthesis of TpPa-1 and TpPa-2 by a cascade Schiff-base-tautomerism reaction.
Figure 6. (A) The reaction mechanism for triazine formation via a cascade Schiff-base-Michael addition reaction. (B) representative structures of CTF-HUST-1-4.
Figure 7. Schematics for the synthesis of benzoxazole-linked COFs (LZU-190, LZU-191, and LZU-192) via cascade reactions.
Figure 8. Posts-synthetic linkage conversation in imine-linked COFs to kinetically lock the reversible bonds. See also in A,[79] B,[80] C,[81] D,[82] E,[83] F,[84] G,[85] H.[86]
Figure 9. (A) Transformation of the imine-linked COF-1 to quinoline-linked MF-1 by an aza-Diels-Alder cycloaddition reaction. (B) PXRD patterns of COF-1 and MF-1a after treatment with various extreme conditions. (C) Contact angles of water droplets on the pressed pellet of COF-1 and MF-1a–e. Reprinted with permission from Li et al.[86] Copyright 2018, Springer Nature.
Figure 10. Synthetic pathway for CAF-1 and CAF-2 via the post-devitrification of amorphous polyamide polymers.
Figure 11. (A) Synthesis of COFs by Schiff-base reaction of aldehyde (TpOMe) and corresponding amines. (B, C) The layered structures of TpOMe-Pa and TpOMe-BD$(NO_2)_2$ (C-grey, N-blue, O-red, and H-white). The interlayer C-H···N and intralayer C-H···O H-bonding based on distances shown with dotted line and angles in degree. Reprinted with permission from Halder et al.[97] Copyright 2018, Wiley-VCH Verlag GmbH & Co. KGaA, Weinheim.
Figure 12. Synthesis of robust (A) TPB-DMTP-COF and (B) TPB-DMeTP-COF. Inset: The structure of the edge units of TPB-DMTP-COF and the resonance effect of the oxygen lone pairs that weaken the polarization of the C=N bonds and soften the interlayer repulsion in COFs.
Figure 13. Schematics of imparting superhydrophobicity on COF-V via the pore-surface modification by a thiol-ene reaction with 1*H*,1*H*,2*H*,2*H*-perfluorodecanethiol.
Figure 14. (A) Schematics of the molecularly defined interface. (B) The mechanism of concerted CO_2 reduction taking place at the interface between COFs and the silver electrode through the critical carbamate formation. Electrons directly transferred to the CO_2 molecules that were activated by the amine linkage of COFs. Reprinted with permission from Liu et al.[85] Copyright 2018, Elsevier Inc.
Figure 15. (A) Synthesis of olefin-linked TFPT-BTAN and TFPT-BTAN-AO COFs. (B) Adsorption isotherm of UO_2^{2+} for TFPT-BTAN-AO and POP-TB-AO (pH 4.0). (C) Adsorption kinetics of UO_2^{2+} for TFPT-BTAN-AO and POP-TB-AO (pH 4.0). (D) The removal efficiency of UO_2^{2+} under different pH conditions. (E) The selective adsorption of the test ions. Error bars represent S.D. n = 3 independent experiments. Reprinted with permission from Cui et al.[49] Copyright 2020, Springer Nature.
Figure 16. The optoelectronic response of PBHP-TAPT COF to HCl and NH_3 vapors by selective protonation and deprotonation of the triazine moieties. Reprinted with permission Kulkarni et al.[37] Copyright 2020, Springer Nature.

Table Title and Legend

Table 1 Summary of representative COFs showing exceptional chemical stability.

COFs	Linkage	Testing Conditions [a]	Duration	Strategy	Year	Reference
Strengthening covalent linkages in COFs						

GS-COF-1 GS-COF-2	Benzofuran	12 M HCl, 14 M NaOH at RT	3 d	Cascade	2020	75
TZ-COFs 1–5	Thiazole	12.5 M HCl (50°C) 14 M KOH at RT 1 M CH_3ONa at RT 1 M $NaBH_4$ at RT Boiling water	2 d	Cascade	2020	72
CoPc-PDQ-COF	Phenazine	DMF, DMSO, THF, MeOH 12 M HCl,14 M NaOH at RT Boiling water	40 d	One-step robust linkage	2020	50
JNU-1	Amide	THF, EtOH, DMF, water 10 M HCl, 1 M NaOH at RT	1 d	Post-linker exchange	2020	87
QH-COF-1 QH-COF-2	Tetrahydro quinoline	Trifluoroacetic acid 12 M HCl, 14 M NaOH 18 M H_2SO_4 at RT	3 d	Cascade	2020	74
B-COF-2 T-COF-2	Thieno[3,2-c]pyridine	12 M HCl, 12 M NaOH at 50 ℃	1 d	Locking linkage	2020	84
S-TmTaDm-COF P-StTaDm-COF	Amine Quinoline	12 M HCl (60°C) 14 M NaOH (60°C) 1 M $NaBH_4$ (60°C) 1 M $KMnO_4$ (RT) Trifluoroacetic acid (RT)	1 d	Cascade	2020	73
TFPT-BTAN-AO	Olefin	1 M HCl, 1 M NaOH 5 M HNO_3 at RT Boiling water, γ-ray irradiation	12 h	One-step robust linkage	2020	49
TTO-COF	Olefin	9 M HCl, 9 M NaOH at RT	1 d	One-step robust linkage	2020	112
PG-BBT BZ-BBT	Thiazole	3 M HCl, 3 M KOH at RT Boiling water	7 d	One-step robust linkage	2020	71
JLU-505 JLU-506	Arylether	12 M HCl, 18 M H_2SO_4 HF (40%), 14 M NaOH MeONa (5 M in MeOH) Chromic acid solution $LiAlH_4$ (2.4 M in THF) at RT	7 d	One-step robust linkage	2019	55
COF-316 COF-318	Arylether	12 M HCl, 14 M NaOH at RT	3 d	One-step robust linkage	2019	33
BO-COF	Oxazole	12 M HCl, 10 M NaOH at RT	3 d	Locking linkage	2019	83
LZU-501 LZU-506	Imidazole	DMF, H_2O 9 M HCl, 9 M NaOH at RT	3 d	Cascade	2019	69
COF-701	Olefin	12.1 M HCl Saturated aqueous methanolic KOH Organolithium reagents at RT	1 d	One-step robust linkage	2019	44

COF-1 COF-2	Olefin	11 M HCl, 12 M NaOH at RT	7 d	One-step robust linkage	2019	43
JUC-520 JUC-521 JUC-522 JUC-523	Ketoenamine	DMF, THF, MeOH, H_2O 1 M HCl, 1 M NaOH at RT	3 d	One-step robust linkage	2019	38
V-COF-1 V-COF-2	Olefin	12 M HCl, 12 M NaOH at RT	4 d	One-step robust linkage	2019	39
g-$C_{34}N_6$-COF	Olefin	12 M HCl 12 M *p*-toluenesulfonic acid 12 M NaOH at RT	3 d	One-step robust linkage	2019	48
Por-*sp*^{2}c-COF	Olefin	DMF, THF, MeOH MeCN, acetone 9 M HCl, 9M NaOH at RT Boiling water	1 d	One-step robust linkage	2019	110
CCP-HATN	Olefin	12 M HCl, 12 M NaOH at RT	7 d	One-step robust linkage	2019	120
TpODH	Hydrazone	9 M HCl, 9 M NaOH at RT Boiling water	2 d	One-step robust linkage	2019	26
TpDTz	Ketoenamine	12 M HCl, boiling water 1 M KOH (3 d)	7 d	One-step robust linkage	2019	58
MF-1a	Quinoline	98% TfOH,12 M HCl at RT 12 M HCl at 100 ºC 14 M NaOH at 100 ºC $KMnO_4$ and $NaBH_4$ at 60 ºC	3 d to 2 months	Locking linkage	2018	86
CAF-1 CAF-2	Amide	1 M HCl at 100 °C 1 M NaOH at 100 °C 12 M HCl, 14 M NaOH at RT	1 or 7 d	Post-devitrification	2018	88
TTT-COF	Thiazole	12.5 M HCl at 50 ºC 12 M KOH at RT 1 M N_2H_4, 1 M $NaBH_4$	16 h	Locking linkage	2018	80
CCOF-6	Amide	12 M HCl, 1 M NaOH at RT	1 d	Locking linkage	2018	118
COF-300-AR	Amine	6 M HCl, 6 M NaOH at RT	12 h	Locking linkage	2018	85
COF-921 LZU-192	Oxazole Thiazole	12.1 M HCl 18 M H_2SO_4 14.8 M H_3PO_4 10 M NaOH at RT	1 d	Cascade	2018	81
LZU-190 LZU-191 LZU-192	Oxazole	9 M HCl, trifluoroacetic acid 9 M NaOH, visible light at RT Boiling water	3 d	Cascade	2018	67
sp^{2}c-COF *sp*^{2}c-COF-2 *sp*^{2}c-COF-3	Olefin	DMF, THF, H_2O, MeOH 12 M HCl, 12 M NaOH at RT	7 d	One-step robust linkage	2018	42
BtaMth	Hydrazone	MeOH, EtOH, IPA, Hexane, H_2O, DCM, THF, DMF 2 M HCl, 2 M NaOH at RT	2 d	One-step robust linkage	2017	27

Amide TPB-TP-COF	Amide	12 M HCl, 1 M NaOH at RT	7 d	Locking linkage	2016	79
3PD	Ketoenamine	9 M HCl, water at 50 ºC	7 d	One-step robust linkage	2016	36
TpPa-1	Ketoenamine	9 M HCl at RT 9 M NaOH at RT (1 d) Boiling water	7 d	Enol-to-keto	2012	30
Tailoring supramolecular noncovalent interactions						
TPB-DMeTP-COF	Imine	12 M HCl, 14 M NaOH at RT H_3PO_4 (0.7 M in THF) CH_3CN, THF, boiling water	7 d	Interlayer reinforcement	2020	99
COF-118	Urea	12 M HCl Saturated $NaHCO_3$ Boiling water	1 d	Intralayer H-bonding	2018	32
TAPB-BMTTPA-COF	Imine	Hexane 6 M HCl, 6 M NaOH at RT Boiling water	3 d	Interlayer reinforcement	2018	115
TpOMe-Pa1 TpOMe-BD$(NO_2)_2$	Imine	12 M HCl, 18 M H_2SO_4 9 M NaOH at RT	7 d	Interlayer H-bonding	2018	97
TPB-DMTP-COF	Imine	DMSO, DMF, THF, MeOH cyclohexanone, boiling water 12 M HCl, 14 M NaOH at RT	7 d	Interlayer reinforcement	2015	98
DhaTab	Imine	3 M HCl Phosphate buffer pH 7.4 Water at RT	7 d	Intralayer H-bonding	2015	96
DhaTph	Imine	3 M HCl, water at RT	7 d	Intralayer H-bonding	2013	95
Manipulating intrinsic properties of linkers						
JUC-530 JUC-531	Imine	DMF, THF, acetone 3 M HCl, 3M H_2SO_4 20 M NaOH at RT Boiling water (30 d)	7 d	Surface Hydrophobicity	2020	105
COF-F6	Hydrazone	HCl (38%), H_3PO_4 (85%) HNO_3 (65%) at RT	1 d	Surface Hydrophobicity	2020	104
BBO-COF	Imine	12 M HCl Trifluoroacetic acid 12 M NaOH at RT Boiling water	7 d	Surface Hydrophobicity	2019	103
Py-COF	Imine	12 M HCl, 12 M NaOH at RT Boiling water	3 d	Surface Hydrophobicity	2019	102
5-^{i}Pr	Imine	0.1 M HCl, water 20 M NaOH at 100 ºC	7 d	Steric hindrance	2018	100
COF-VF	Imine	12 M HCl, 14 M NaOH at RT Boiling water	7 d	Surface Hydrophobicity	2018	106
COF-DTF	Imine	12 M HCl, 14 M NaOH at RT Boiling water	7 d	Surface Hydrophobicity	2018	117

[a] DMSO: Dimethyl sulfoxide; THF: Tetrahydrofuran; TfOH: Triflic acid; IPA, Isopropanol; MeCN: Acetonitrile; DCM: Dichloromethane; DMF: Dimethylformamide; RT: Room temperature.

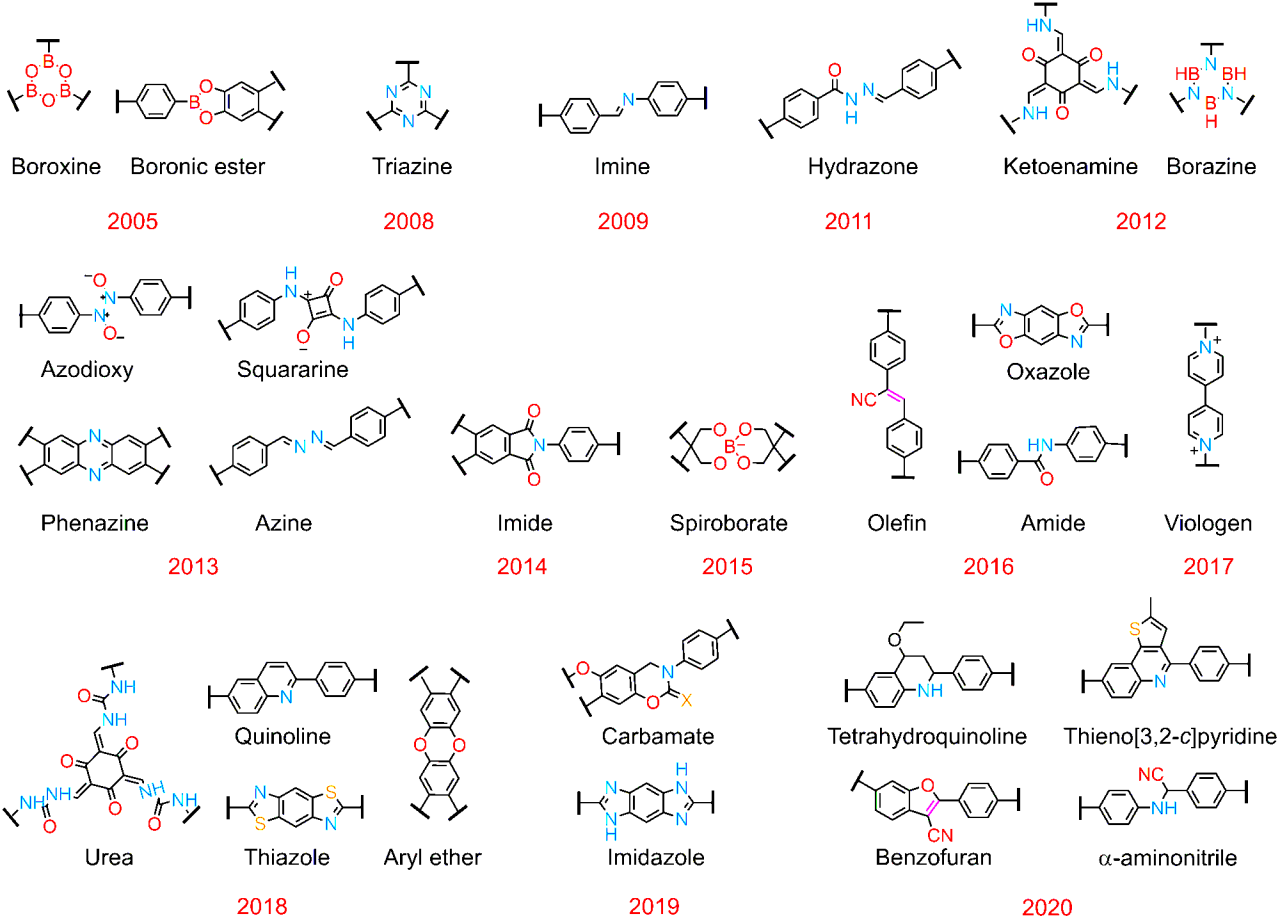
Boroxine
Boronic ester
Triazine
Imine
Hydrazone
Ketoenamine
Borazine
2005
2008
2009
2011
2012
Azodioxy
Squararine
Oxazole
Phenazine
Azine
Imide
Spiroborate
Olefin
Amide
Viologen
2013
2014
2015
2016
2017
Quinoline
Carbamate
Tetrahydroquinoline
Thieno[3,2-c]pyridine
Urea
Thiazole
Aryl ether
Imidazole
Benzofuran
α-aminonitrile
2018
2019
2020

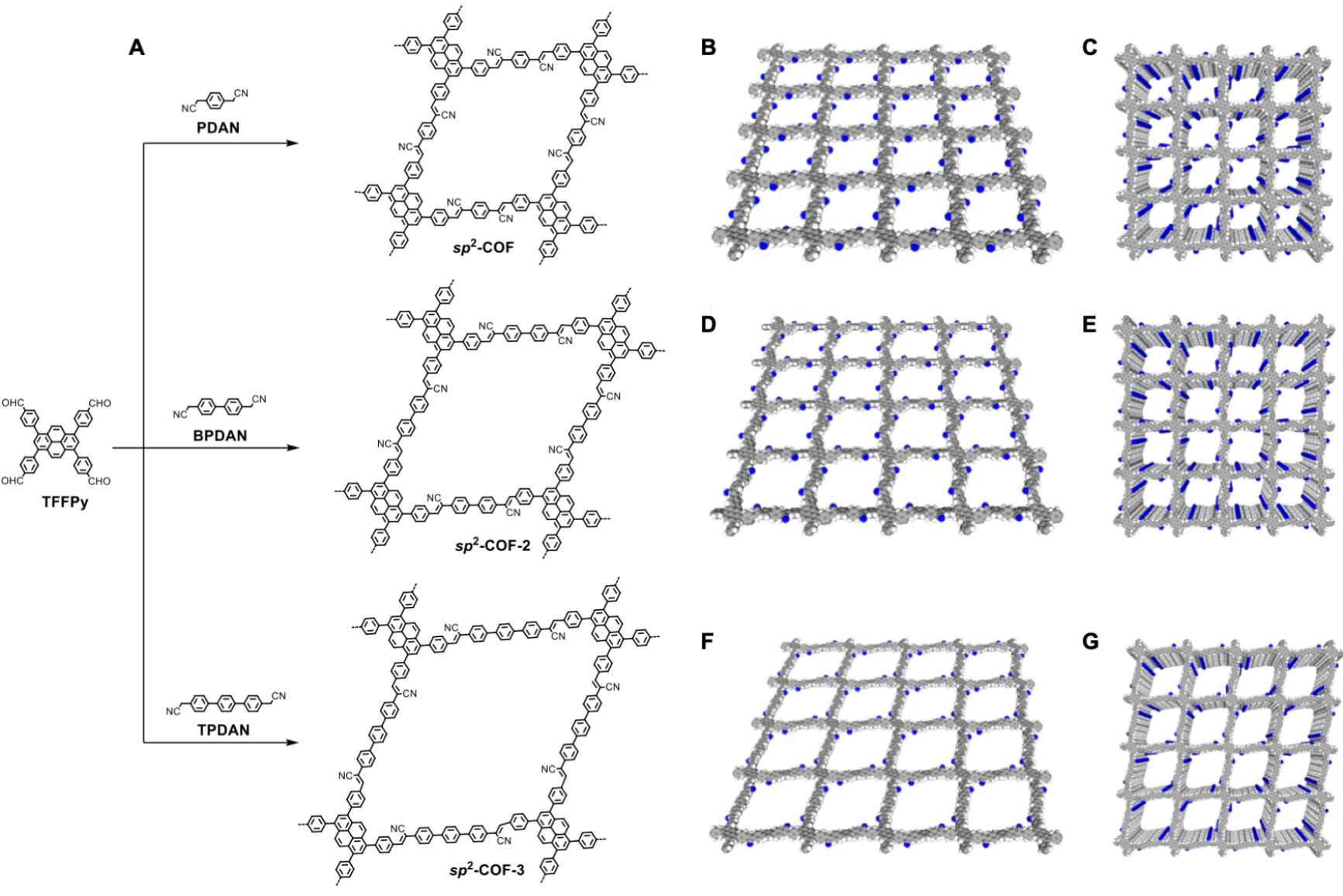
A
PDAN
BPDAN
TPDAN
TFFPy
sp2-COF
sp2-COF-2
sp2-COF-3
B
C
D
E
F
G

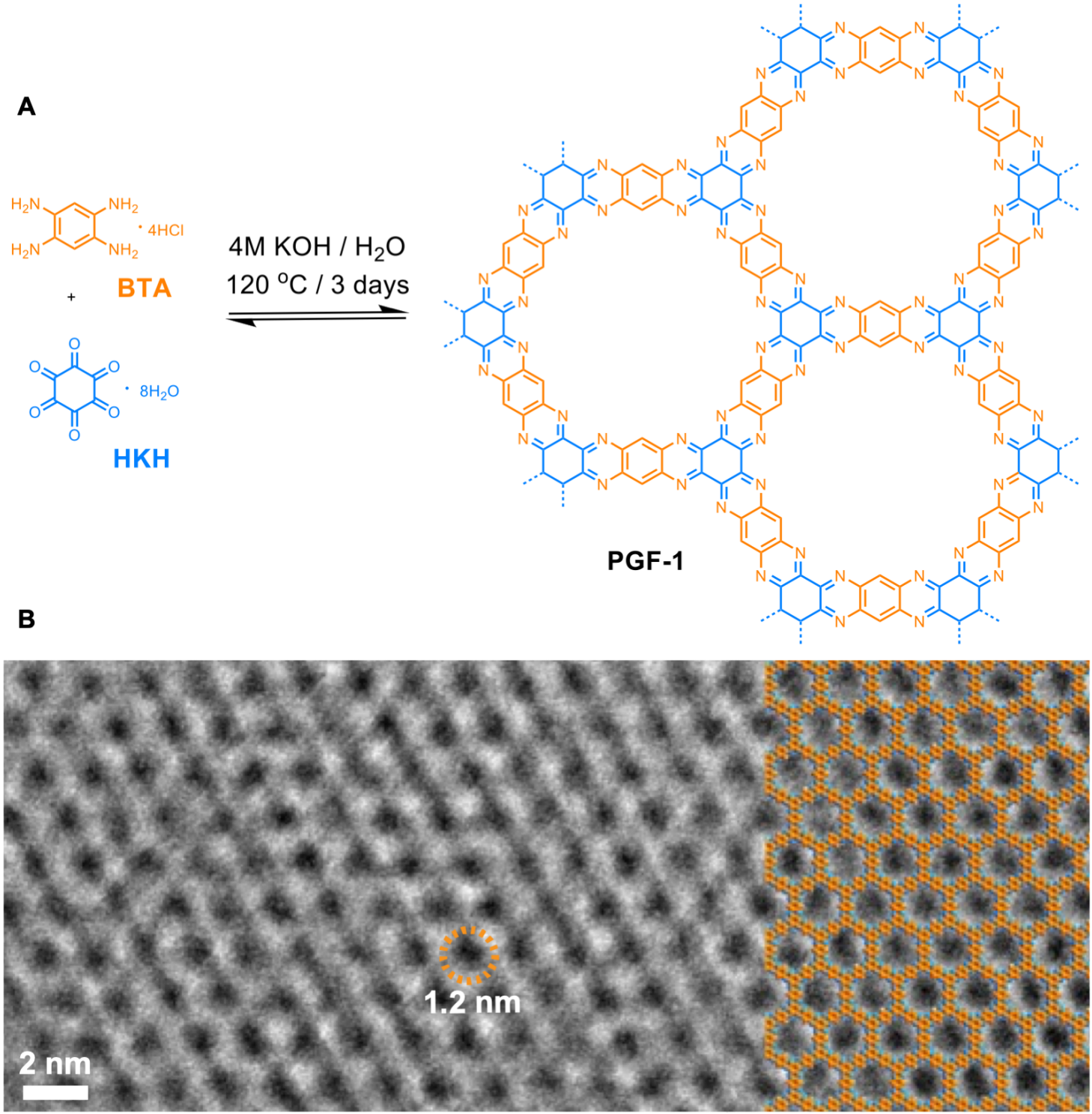
A
BTA
HKH
4M KOH / H2O
120 °C / 3 days
PGF-1
B
1.2 nm
2 nm

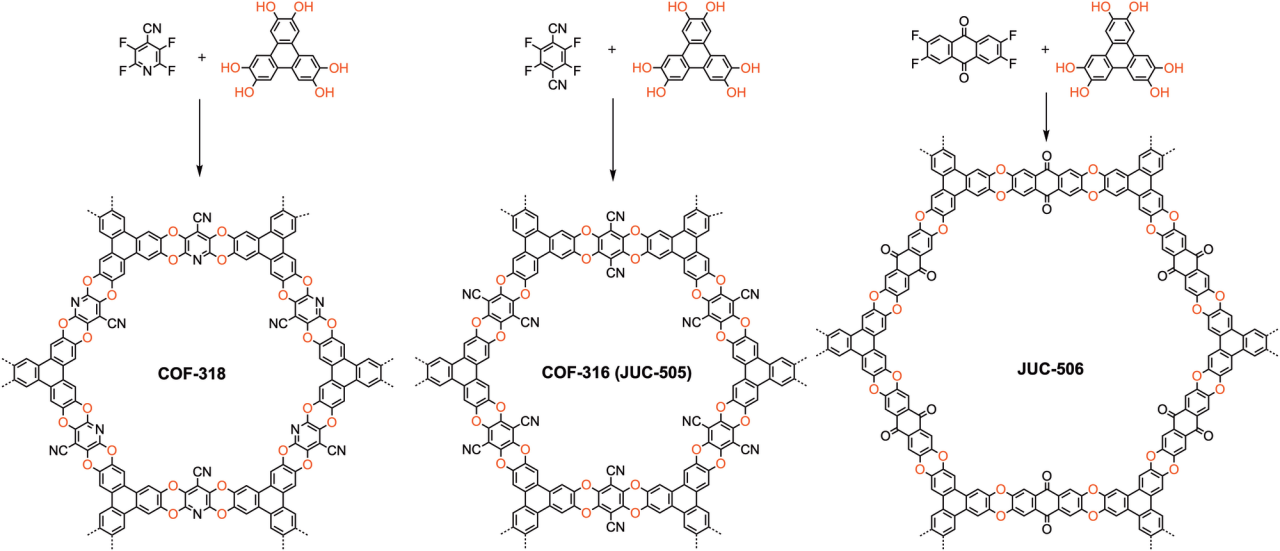
COF-318
COF-316 (JUC-505)
JUC-506

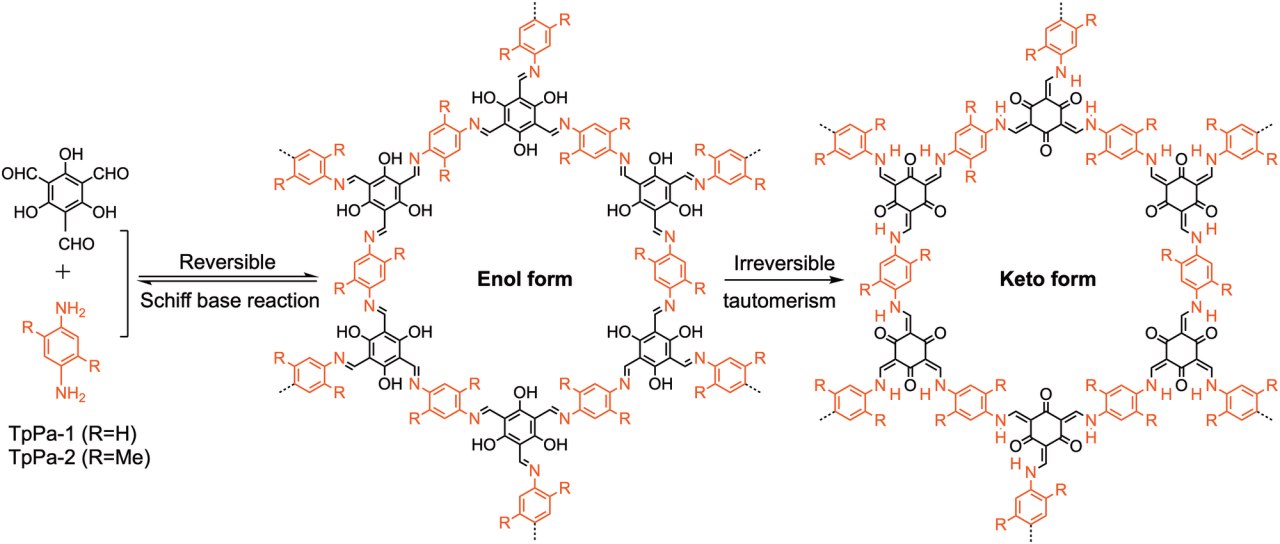
Reversible
Schiff base reaction
Enol form
Irreversible
tautomerism
Keto form
TpPa-1 (R=H)
TpPa-2 (R=Me)

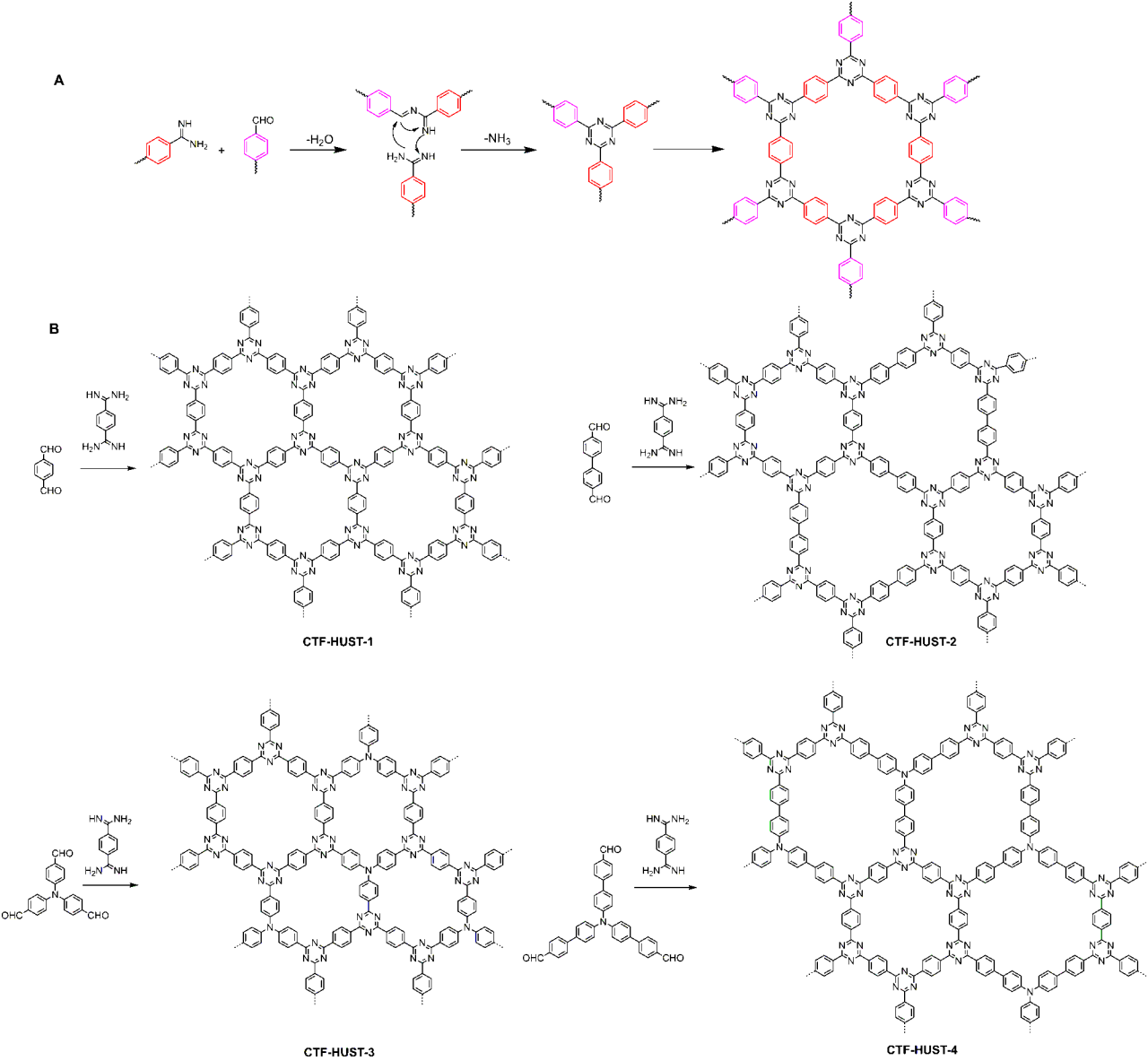
A
-H2O
-NH3
B
CTF-HUST-1
CTF-HUST-2
CTF-HUST-3
CTF-HUST-4

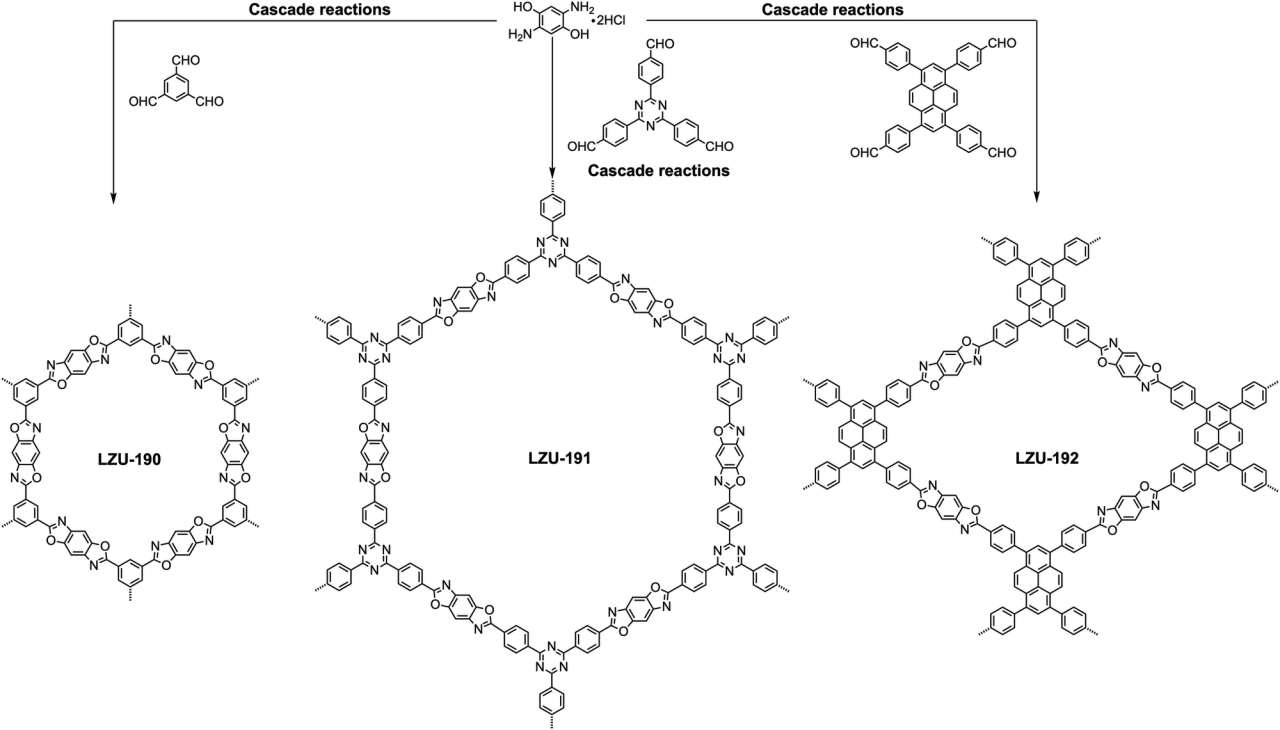
Cascade reactions
Cascade reactions
Cascade reactions
•2HCl
LZU-190
LZU-191
LZU-192

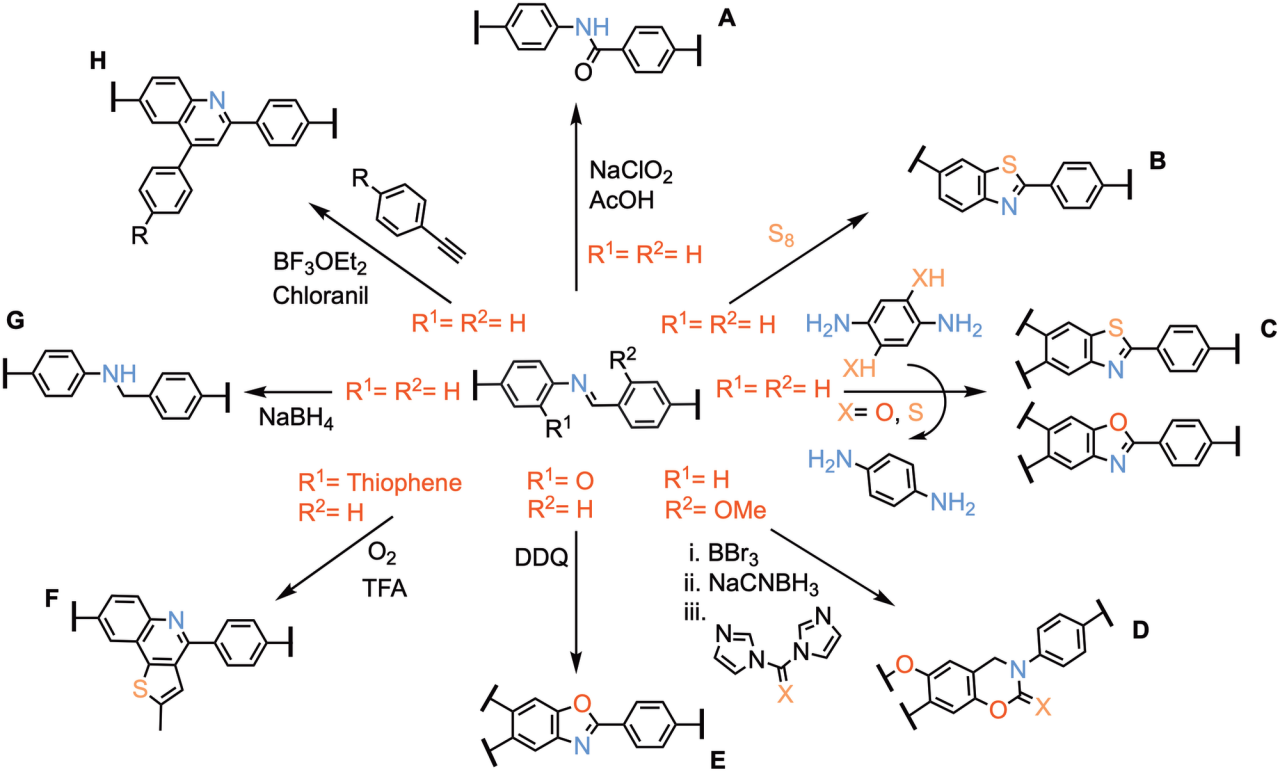
A
NaClO2
AcOH
R1= R2= H
B
S8
R1= R2= H
C
XH
H2N
NH2
XH
X= O, S
H2N
NH2
R1= R2= H
G
NaBH4
R1= R2= H
R2
N
R1
H
R
R
BF3OEt2
Chloranil
R1= R2= H
R1= Thiophene
R2= H
O2
TFA
F
R1= O
R2= H
DDQ
E
R1= H
R2= OMe
i. BBr3
ii. NaCNBH3
iii.
X
D

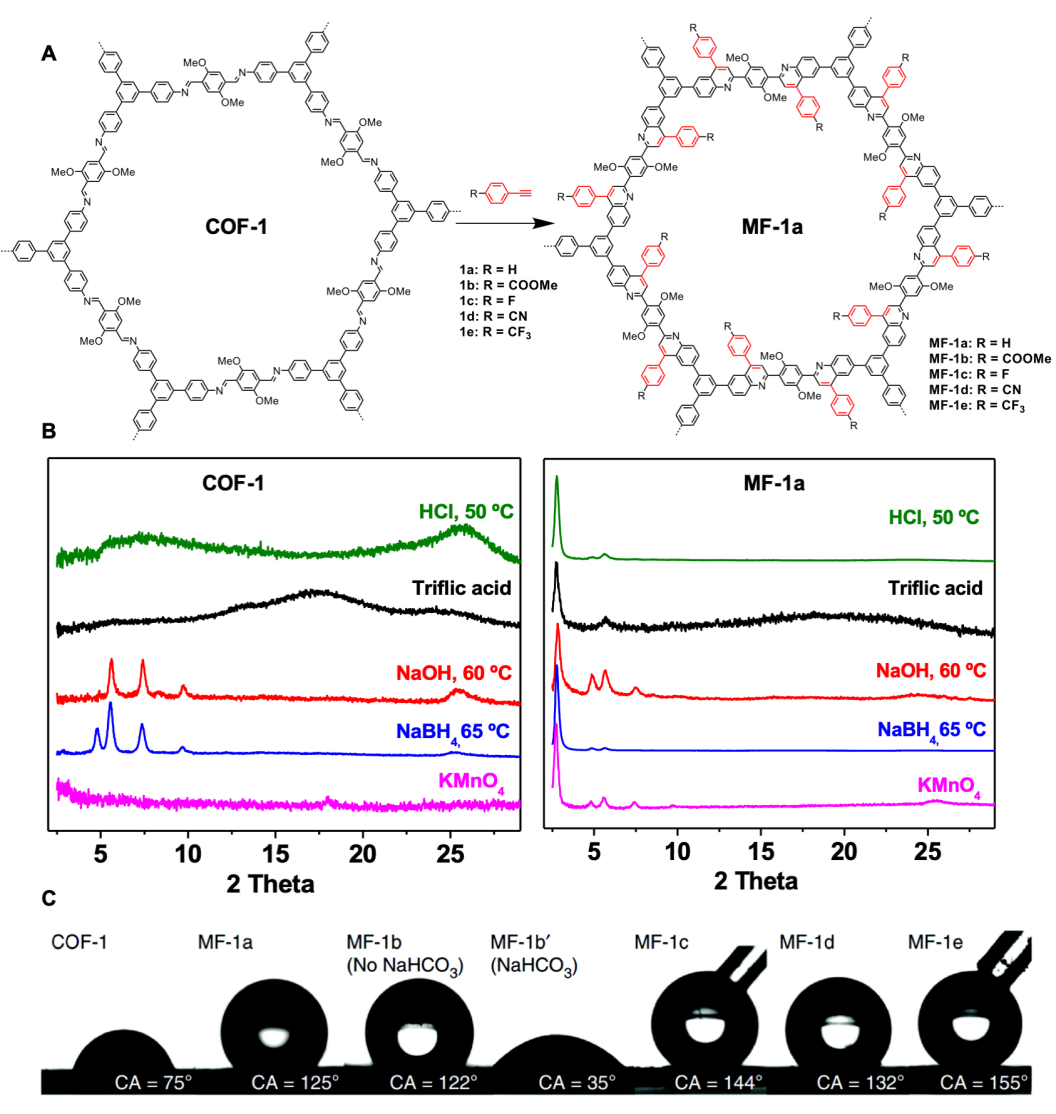
A
COF-1
1a: R = H
1b: R = COOMe
1c: R = F
1d: R = CN
1e: R = CF3
MF-1a
MF-1a: R = H
MF-1b: R = COOMe
MF-1c: R = F
MF-1d: R = CN
MF-1e: R = CF3
B
COF-1
HCl, 50 ºC
Triflic acid
NaOH, 60 ºC
NaBH4, 65 ºC
KMnO4
2 Theta
MF-1a
HCl, 50 ºC
Triflic acid
NaOH, 60 ºC
NaBH4, 65 ºC
KMnO4
2 Theta
C
COF-1
MF-1a
MF-1b (No NaHCO3)
MF-1b′ (NaHCO3)
MF-1c
MF-1d
MF-1e
CA = 75°
CA = 125°
CA = 122°
CA = 35°
CA = 144°
CA = 132°
CA = 155°

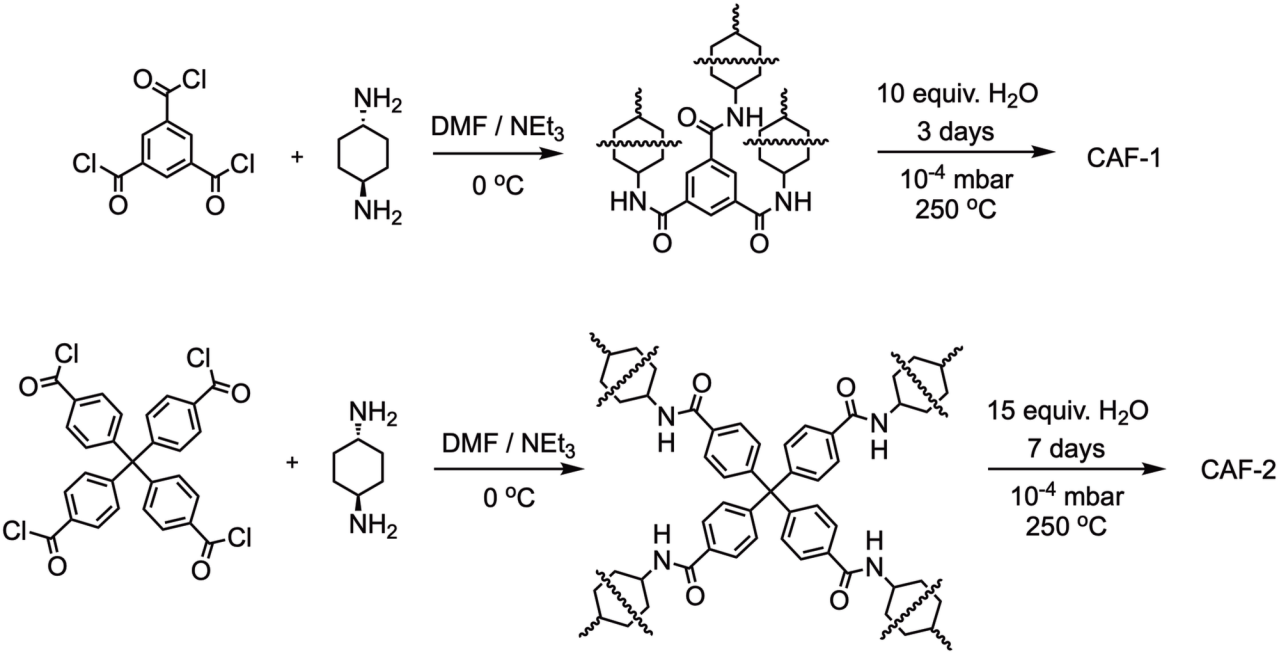
DMF / NEt3
0 °C
10 equiv. H2O
3 days
10-4 mbar
250 °C
CAF-1
DMF / NEt3
0 °C
15 equiv. H2O
7 days
10-4 mbar
250 °C
CAF-2

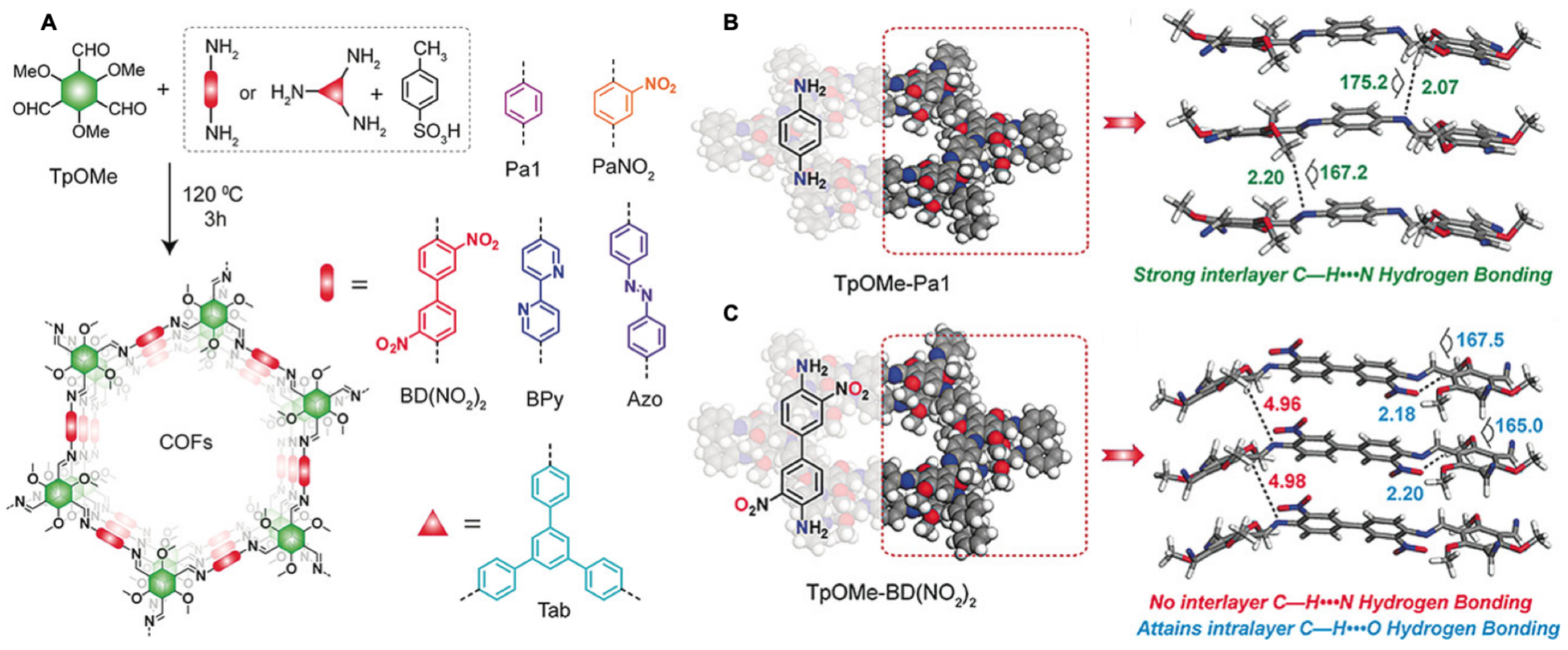
A
TpOMe
120 °C
3h
COFs
or
Pa1
PaNO2
BD(NO2)2
BPy
Azo
Tab
B
TpOMe-Pa1
175.2
2.07
2.20
167.2
Strong interlayer C—H•••N Hydrogen Bonding
C
TpOMe-BD(NO2)2
167.5
4.96
2.18
165.0
4.98
2.20
No interlayer C—H•••N Hydrogen Bonding
Attains intralayer C—H•••O Hydrogen Bonding

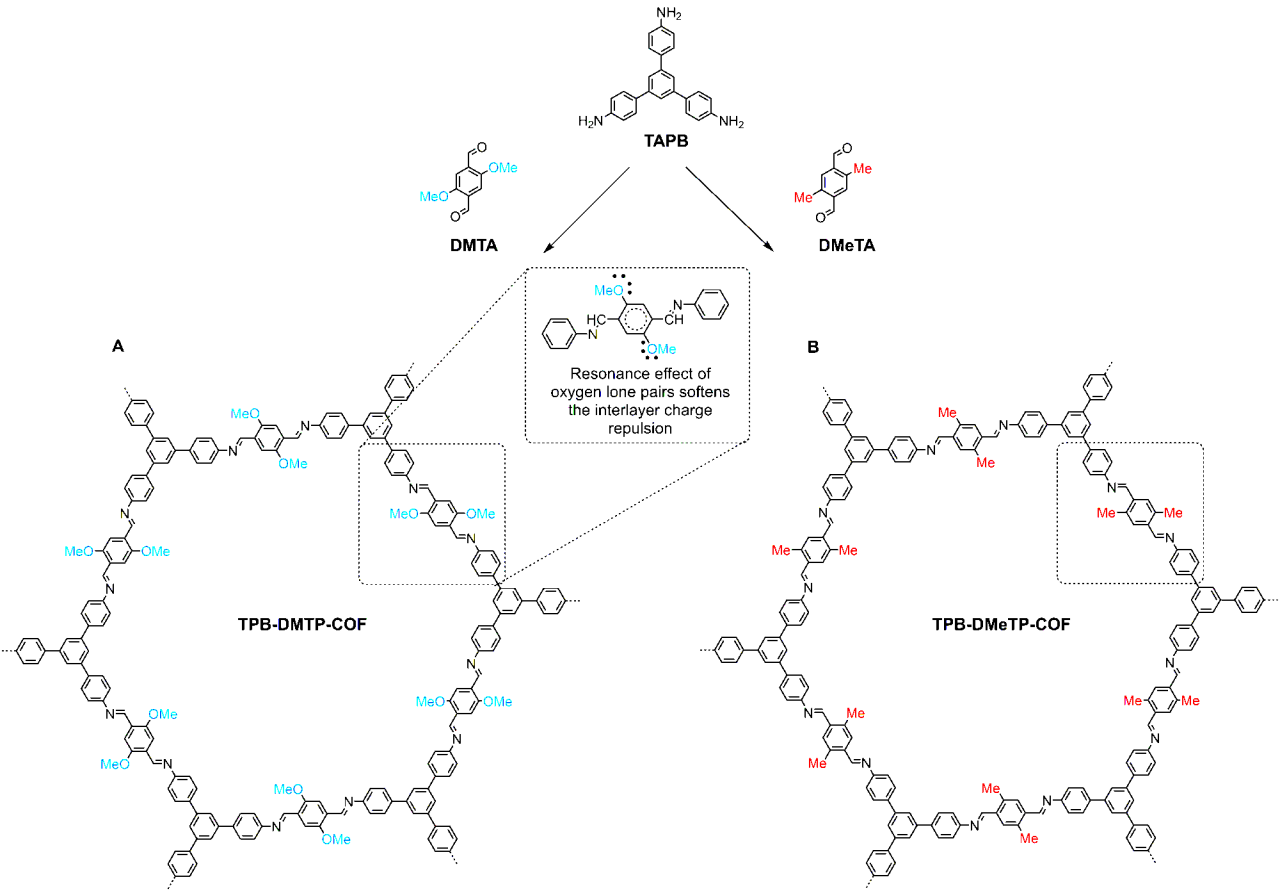
TAPB
DMTA
DMeTA
Resonance effect of oxygen lone pairs softens the interlayer charge repulsion
A
B
TPB-DMTP-COF
TPB-DMeTP-COF

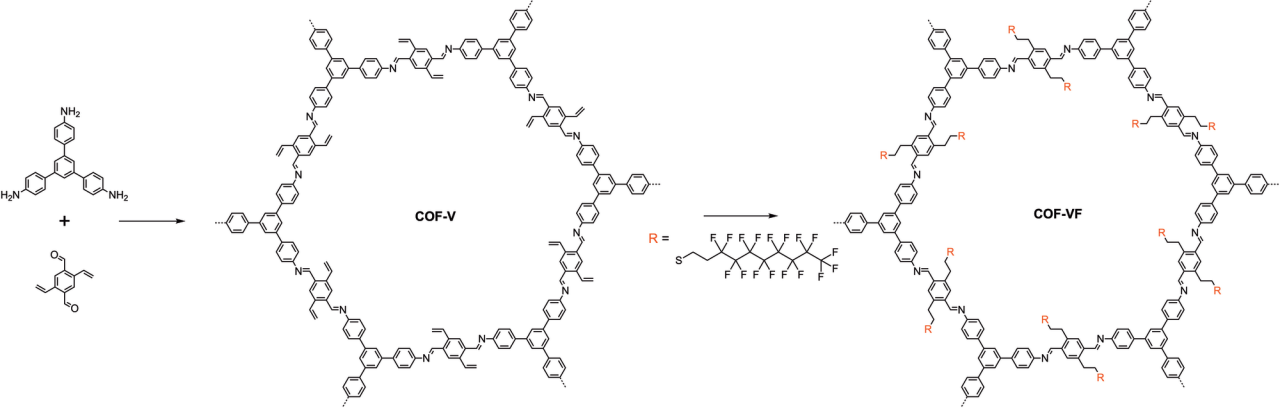
NH2
NH2
NH2
+
O
O
COF-V
R =
S
F
COF-VF
R

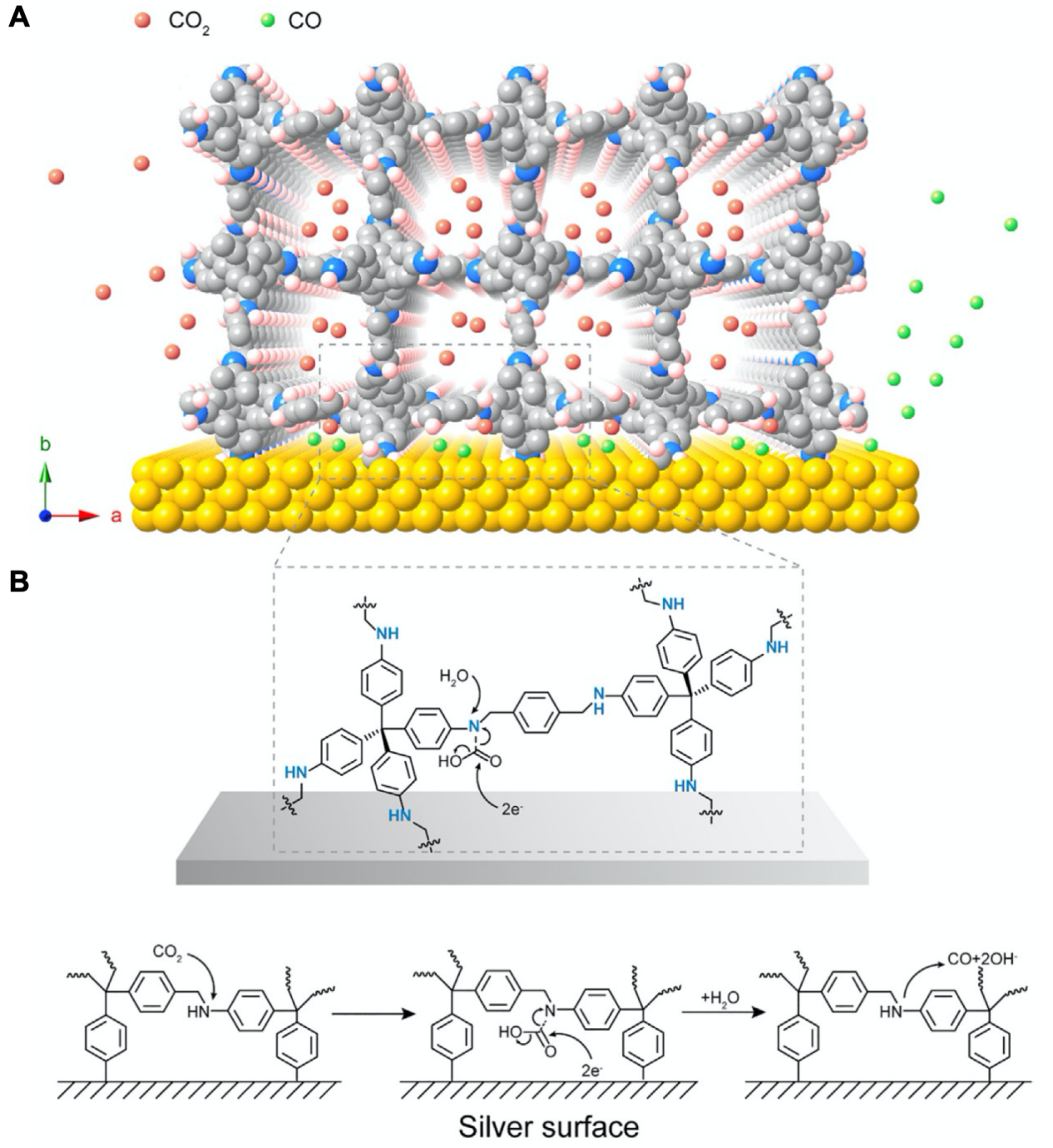
A
CO2
CO
b
a
B
NH
H2O
N
H
HO
O
2e-
HN
CO2
+H2O
CO+2OH-
Silver surface

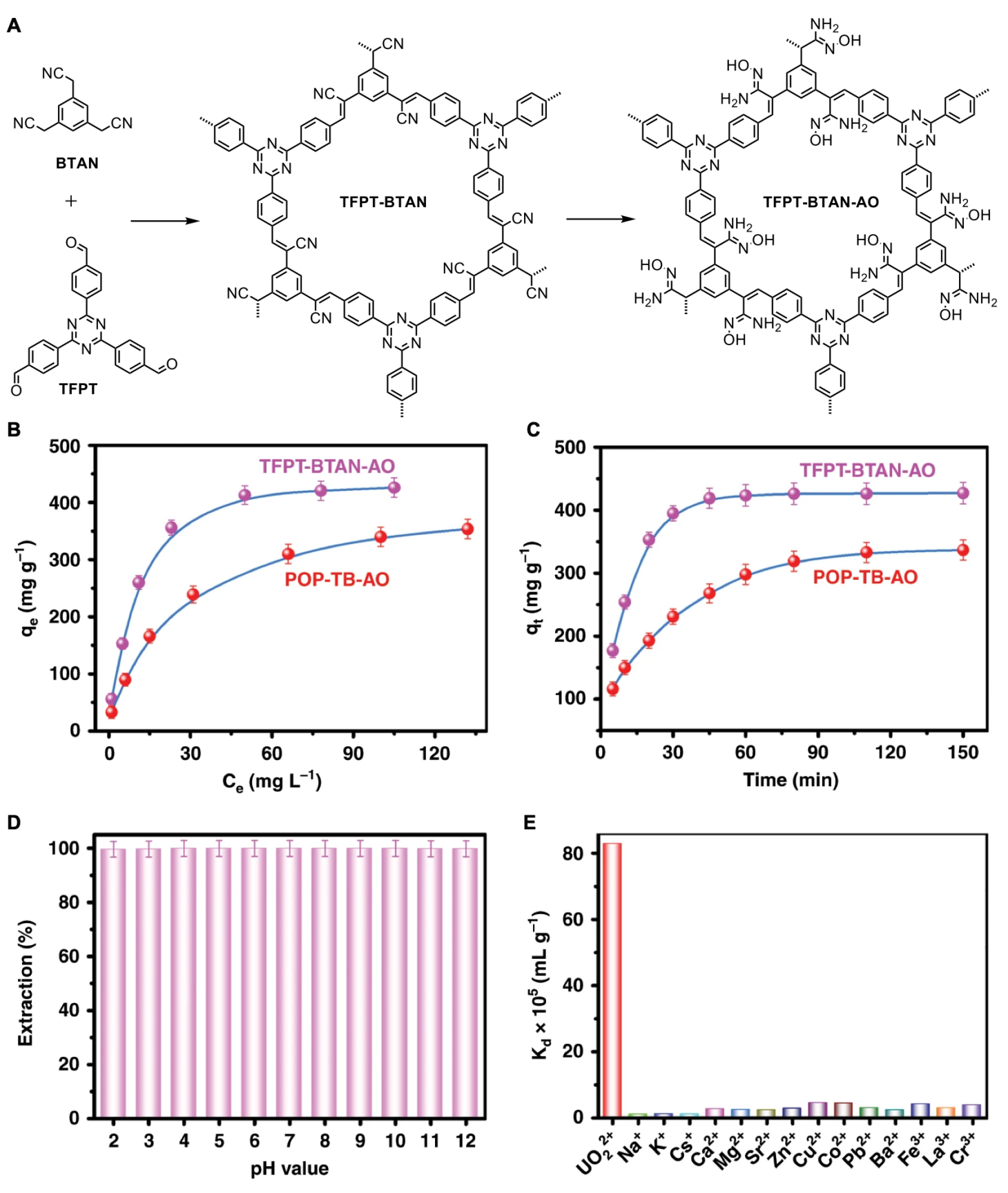
A
BTAN
TFPT
TFPT-BTAN
TFPT-BTAN-AO
B
TFPT-BTAN-AO
POP-TB-AO
q_e (mg g^{-1})
C_e (mg L^{-1})
C
TFPT-BTAN-AO
POP-TB-AO
q_t (mg g^{-1})
Time (min)
D
Extraction (%)
pH value
E
$K_d \times 10^5$ (mL g^{-1})
UO_2^{2+} Na^+ K^+ Cs^+ Ca^{2+} Mg^{2+} Sr^{2+} Zn^{2+} Cu^{2+} Co^{2+} Pb^{2+} Ba^{2+} Fe^{3+} La^{3+} Cr^{3+}

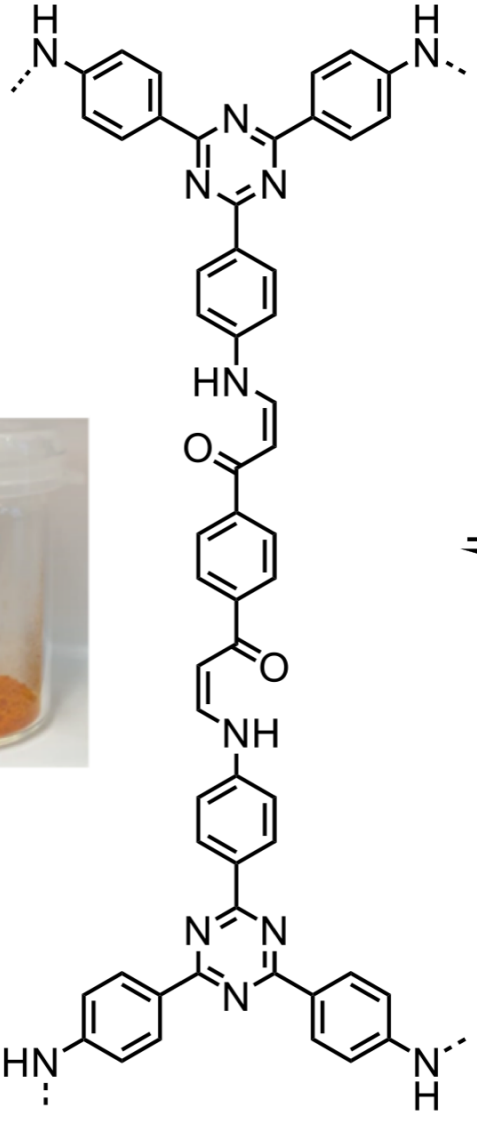

HCl

NH_3